11-22-1999

Thermodynamic Model and the Controlling Variables of Phosphate Lattice Loss

Mohammad Abutayeh
University of South Florida

Graduate School
University of South Florida
Tampa, Florida

CERTIFICATE OF APPROVAL

Master's Thesis

This is to certify that the Master's Thesis of

MOHAMMAD ABUTAYEH

with a major in Chemical Engineering has been approved by
the Examining Committee on November 22, 1999
as satisfactory for the thesis requirement
for the Master of Science in Chemical Engineering degree

Examining Committee:

Major Professor: J. Carlos Busot, Ph.D.

Co-Major Professor: Luis H. Garcia-Rubio, Ph.D.

Member Professor: Scott W. Campbell, Ph.D.

THERMODYNAMIC MODEL AND THE CONTROLLING VARIABLES OF PHOSPHATE LATTICE LOSS

by

MOHAMMAD ABUTAYEH

A thesis submitted in partial fulfillment
of the requirements for the degree of
Master of Science in Chemical Engineering
Department of Chemical Engineering
College of Engineering
University of South Florida

December 1999

Major Professor: J. Carlos Busot, Ph.D.

ACKNOWLEDGEMENTS

I would like to first thank God for giving me the patience and the strength to complete this work. Then, I wish to express my deepest appreciation to my major professor, Dr. J. Carlos Busot, for his valuable criticism and professional guidance. I would also like to express my gratitude to my co-major professor, Dr. L. Garcia-Rubio, for encouraging and providing me with the opportunity to continue my graduate studies. I must also thank my committee member professor, Dr. Scott W. Campbell, for his support and tremendous knowledge that guided me throughout my academic years.

Last but not least, I like to extend my deepest appreciation to my family and friends for their support and motivation throughout my years of education in general and to Cargill Fertilizer, Inc. for generously supporting this project.

TABLE OF CONTENTS

LIST OF TABLES

LIST OF FIGURES

LIST OF SYMBOLS

$\%H_2SO_4$	Percent H_2SO_4 Equivalence by Mass in Liquid [Kg H_2SO_4/Kg Liquid]
$\%P_2O_5$	Percent P_2O_5 Equivalence by Mass in Liquid [Kg P_2O_5/Kg Liquid]
$\%P_2O_5^{(S)}$	Percent P_2O_5 Equivalence by Mass in Solid [Kg P_2O_5/Kg Solid]
A	Debye-Hückel Constant
a_i	Activity of Species i [mol i/Kg H_2O]
B^+, B^-	Bromley's Interaction Parameter Components
B_i	Bromley's Interaction Parameter of Species i
B_{ij}	Bromley's Interaction Parameter of Species i
Cp_i	Partial Molar Specific Heat of Species i [J/(mol i·K)]
F_i	Summation of Bromley's Interaction Parameters of Species i
f_i	Fugacity of Vapor Species i
G_i	Partial Molar Gibbs Free Energy of Species i [J/mol i]
H_i	Partial Molar Enthalpy of Species i [J/mol i]
I	Ionic Strength [mol/Kg H_2O]
K	Dissolution Equilibrium Constant
Kaq	Vapor-Liquid Equilibrium Constant
Ksp	Solubility Product
M_i	Mass of Species i Per Mass of Water [Kg i/Kg H_2O]
m_i	Molality of Species i [mol i/Kg H_2O]

MW_i	Molecular Weight of Species i [Kg i/mol i]
n_i	Number of Moles of Species i [mol i]
P	Total Pressure [Pa]
P_i	Partial Pressure of Species i [Pa]
pH	Liquid Phase pH
R	Ideal Gas Constant [J/(mol·K)]
r_i	Effective Ionic Radius of Species i [Σ]
T	Temperature [K]
TPM	Total Phosphate Molality [mol TPM/Kg H_2O]
TSM	Total Sulfate Molality [mol TSM/Kg H_2O]
x_i	Mole Fraction of Species i in Solid [mol i/mol Solid]
Z_{ij}	Bromley's Interaction Parameter of Species i
z_i	Ionic Charge of Species i [e]
β	Debye-Hückel Constant
γ_i	Activity Coefficient of Species i
δ^+, δ	Bromley's Interaction Parameter Components
μ_i	Chemical Potential of Species i [J/mol i]
ν_i	Stoichiometric Coefficient of Species i [J/mol i]
ρ_{H2O}	Reference State Density of Water [Kg H_2O/L]
ω_i	Mass Fraction of Species i in Solid [Kg i/Kg Solid]
ΔCp	Molar Specific Heat of Dissolution or Solubility [J/(mol·K)]
ΔG	Molar Gibbs Free Energy of Dissolution or Solubility [J/mol]
ΔH	Molar Enthalpy of Dissolution or Solubility [J/mol]

Θ_{H2SO4}	Moles H_2SO_4 Equivalence Per Moles of TSM [mol H_2SO_4/mol TSM]
Θ_{P2O5}	Moles P_2O_5 Equivalence Per Moles of TPM [mol P_2O_5/mol TPM]
Φ_{H2O}	Mass Fraction of Water in Liquid [Kg H_2O/Kg Liquid]
Ψ_{P2O5}	Moles P_2O_5 Equivalence Per Moles of DCPD [mol P_2O_5/mol DCPD]

Superscripts

+	Proton Charge [+ e = + 1.60217733(49) 3 10^{-19} C]
-	Electron Charge [- e = - 1.60217733(49) 3 10^{-19} C]
o	Reference State Property
L	Liquid Phase Property
S	Solid Phase Property
V	Vapor Phase Property

THERMODYNAMIC MODEL AND THE CONTROLLING VARIABLES OF PHOSPHATE LATTICE LOSS

by

MOHAMMAD ABUTAYEH

An Abstract

Of a thesis submitted in partial fulfillment
of the requirements for the degree of
Master of Science in Chemical Engineering
Department of Chemical Engineering
College of Engineering
University of South Florida

December 1999

Major Professor: J. Carlos Busot, Ph.D.

A thermodynamic model was developed based upon five equilibrium reactions to predict the limits of distribution of phosphates between the liquid and the solid phases in a reactor used to extract phosphoric acid from phosphate rock. A computer code was generated to carry out different simulations of the model using several inputs of temperatures and liquid phase sulfuric acid contents. Ideal Solution, Debye-Hückel, and Robinson-Guggenheim-Bates electrolyte activity coefficient models were employed alternately in each simulation to complete the thermodynamic model and the outputs were compared to one another.

Experimental data of equilibrium constants were regressed to adjust the values of ΔCp° and ΔH° used in the simulations to obtain a more accurate representation of the thermodynamic equilibrium. Results for ionic strength, liquid phase *pH*, and phosphate lattice loss were used to analyze temperature and liquid phase sulfuric acid content effects on the reacting system.

Completing the thermodynamic model with Ideal Solution and Debye-Hückel electrolyte activity coefficient models was found to bind all predictions of phosphate lattice loss. The model prediction of phosphate losses was found to give a lower bound to the real phosphate losses. Furthermore, decreasing temperature and increasing liquid phase sulfuric acid content was found to minimize phosphate lattice loss.

Abstract Approved: _____

Major Professor: J. Carlos Busot, Ph.D.
Professor, Department of Chemical Engineering

Date Approved: _____

CHAPTER 1. INTRODUCTION

1.1 Phosphoric Acid Manufacturing

According to the Dictionary of Chemistry [1], phosphoric acid, also known as orthophosphoric acid, is a water-soluble transparent crystal melting at 42°C. It is used in fertilizers, soft drinks, flavor syrups, pharmaceuticals, animal feeds, water treatment, and to pickle and rust-proof metals.

The dihydrate process is the most common process in the industrial manufacture of phosphoric acid used by the Florida fertilizer plants. As shown in Figure 1, phosphate rock ($Ca_3(PO_4)_2$) is grounded into small granules to facilitate its transport and to increase its reaction surface area. The granules are then sent to a large Continuous Stirred Tubular Reactor (CSTR) along with sulfuric acid (H_2SO_4) and water (H_2O) where the following reaction is carried out:

$$Ca_3(PO_4)_2 + 3H_2SO_4 + 6H_2O \longrightarrow 2H_3PO_4 + 3CaSO_4 \cdot 2H_2O$$

The reaction products, phosphoric acid (H_3PO_4) and gypsum ($CaSO_4 \cdot 2H_2O$) as well as the unreacted reactants and byproducts, are sent to a filter then to a clarifier to separate phosphoric acid from the solid gypsum. Excess water is used in the filter to wash off phosphoric acid from gypsum and to obtain the desired concentration of phosphoric acid. Some of the reactor slurry is recycled back to the reactor from the clarifier for further extraction of phosphoric acid [2].

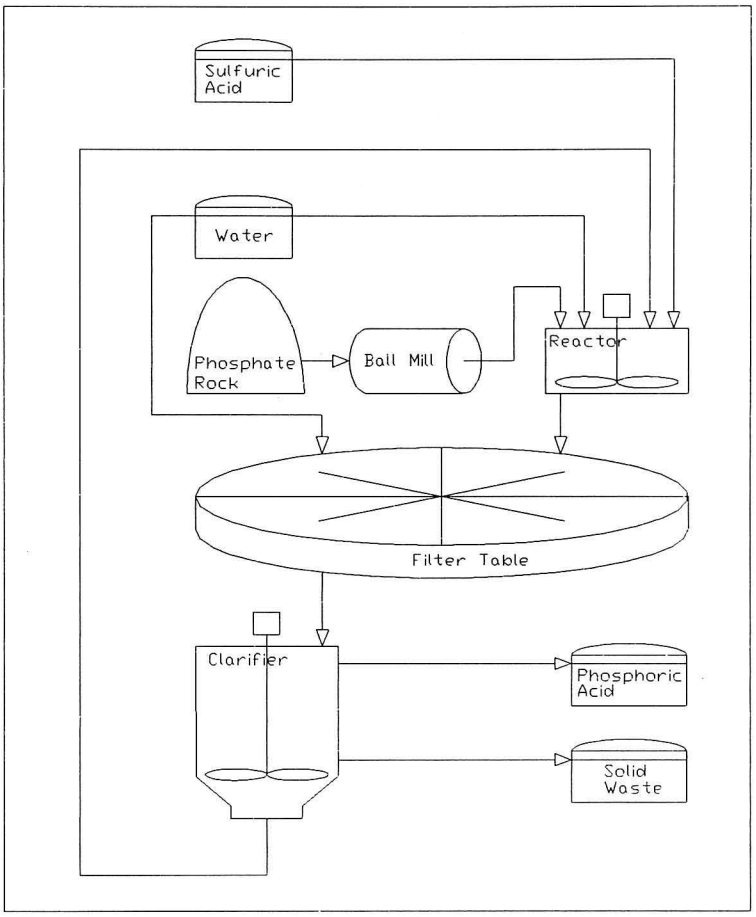

Figure 1. Flowsheet of a Phosphoric Acid Manufacturing Process

1.2 Phosphate Losses

The optimization of the process of manufacturing phosphoric acid can take several paths, one of which is the minimization of phosphate loss. Phosphate loss can occur in many ways and is mainly attributed to the formation of gypsum crystals. The extraction of phosphoric acid from phosphate rock in the dihydrate process involves the formation of gypsum crystals, shown in Figure 2, as a reaction product in the CSTR.

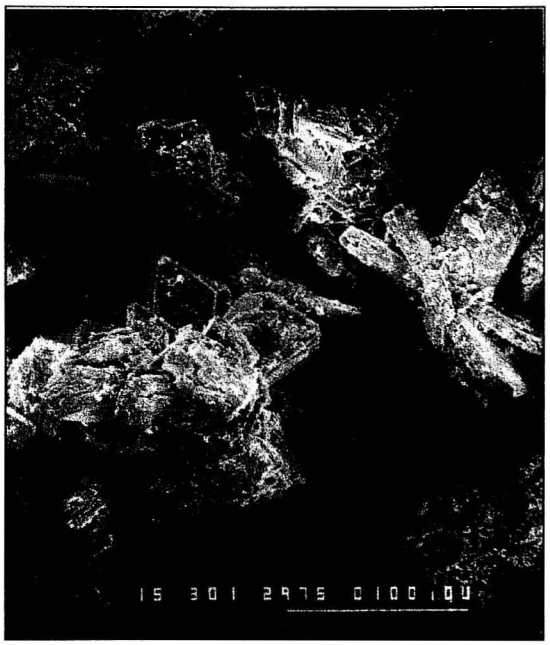

Figure 2. Gypsum Crystals. Shown Bar's Length is 100 microns

One type of phosphate loss takes place during the filtering of the reaction slurry where some of the phosphoric acid fails to wash away from the solid filter cake. This type of loss can be avoided by increasing the filter size or by using excess washing water to improve the filtering process.

A second type of phosphate loss occurs due to poor mixing of the reactor contents. When phosphate rock encounters a local high concentration of sulfuric acid, gypsum will crystallize very rapidly because of the very fast reaction between phosphate rock and sulfuric acid. Gypsum will precipitate covering the unreacted rock granules and forming crystals with an inner core of unutilized phosphates, which is lost as a solid waste. This problem can be overcome by improving the mixing mechanism to eliminate the local over-concentrated zones in the reactor.

A third type of loss arises from the formation of dicalcium phosphate dihydrate or DCPD ($CaHPO_4 \cdot 2H_2O$). Gypsum and DCPD have almost the same molecular weight and density; moreover, they share the same monoclinic crystal lattice structure, which will facilitate the formation of a solid solution of both crystals. Fröchen and Becker [3] confirmed the existence of the DCPD-Gypsum solid solution in 1959. This lattice loss is thermodynamically controlled and the controlling variables will be investigated to determine their effect on that loss.

1.3 Thermodynamic Model of Phosphate Lattice Loss

Thermodynamics can not yield any information about the intermediate states of a given reacting system. These intermediate states are the subject matter of chemical kinetics, which studies reaction rates and mechanisms. Chemical kinetics will predict what chemicals are present while thermodynamics will predict the limits of distribution of those chemicals in the different phases [4].

The objective of this study is to produce a thermodynamic model that will predict the limits of distribution of phosphates between the liquid and the solid phases in the reactor used to extract phosphoric acid from phosphate rock. Different electrolyte activity coefficient models will be employed alternately to complete the model and to carry out different simulations using several inputs of temperatures and liquid phase sulfuric acid contents to study their effect on the distribution of phosphates. The results will then be compared to other literature data to validate the model and assess its accuracy.

CHAPTER 2. THERMODYNAMICS OF ELECTROLYTE SOLUTIONS

2.1 Ionic Equilibrium

It is generally more convenient in aqueous solution thermodynamics to describe the chemical potential of a species i in terms of its activity, a_i. G. N. Lewis [5] defined the chemical potential of species i in terms of its activity as

$$\mu_i(T) = \mu_i^\circ(T) + RT\ln(a_i) \tag{1}$$

A criterion for any given reaction occurring at equilibrium is the minimization of the stoichiometric sum of the chemical potential of the reacting species. This can be represented in a generalized form as

$$\sum_i \nu_i \mu_i(T) = 0 \tag{2}$$

By substituting (1) into (2)

$$\sum_i \nu_i \mu_i^\circ(T) + \sum_i \nu_i RT\ln(a_i) = 0 \tag{3}$$

Further simplification yields

$$\sum_i \nu_i \mu_i^\circ(T) + RT\sum_i \ln(a_i)^{\nu_i} = 0 \tag{4}$$

But $\Sigma_i ln(a_i)^\nu$ is the same as $ln\Pi_i(a_i)^\nu$. Substituting

$$\sum_i \nu_i \mu_i^\circ(T) + RT\ln\prod_i (a_i)^{\nu_i} = 0 \tag{5}$$

Solving for $\Pi_i(a_i)^\nu$

$$\prod_i (a_i)^{\nu_i} = \exp\left(\frac{-\sum_i \nu_i \mu_i^\circ(T)}{RT}\right) \tag{6}$$

The thermodynamic equilibrium constant for a specific reaction is defined as

$$K = \exp\left(\frac{-\sum_i \nu_i G_i^\circ(T)}{RT}\right) \tag{7}$$

The partial molar Gibbs free energy is defined as the reference state chemical potential. Using this definition, Equation (6) and Equation (7) can be equated and the thermodynamic equilibrium constant becomes

$$K = \prod_i (a_i)^{\nu_i} = \exp\left(\frac{-\sum_i \nu_i G_i^\circ(T)}{RT}\right) \tag{8}$$

Values of the partial molar Gibbs free energy for different chemicals are available in the literature as tabulations of the standard Gibbs free energy of formation.

To study the temperature effect on the equilibrium constant, Equation (8) is rewritten to simplify its differentiation

$$\ln K = \frac{-\sum_i \nu_i G_i^\circ(T)}{RT} \tag{9}$$

Differentiating

$$R\frac{d\ln K}{dT} = \frac{d\left(\sum_i \nu_i G_i^\circ(T) \Big/ T\right)}{dT} \tag{10}$$

By definition

$$dG = \frac{\partial G}{\partial T}dT + \frac{\partial G}{\partial P}dP + \frac{\partial G}{\partial n_i}dn_i \tag{11}$$

At constant pressure and composition

$$\frac{\partial}{\partial T}\left(\frac{\sum_i \nu_i G_i^\circ(T)}{T}\right) = \frac{d}{dT}\left(\frac{\sum_i \nu_i G_i^\circ(T)}{T}\right) \tag{12}$$

The Gibbs-Helmholtz relationship [5] is used frequently to show the temperature dependencies of various derived properties. It is given by

$$\left(\frac{\partial G/T}{\partial T}\right)_P = \frac{-H}{T^2} \tag{13}$$

Using Equations (12) and (13), Equation (10) can be restated as

$$R\frac{d\ln K}{dT} = \frac{\sum_i \nu_i H_i(T)}{T^2} \tag{14}$$

This is known as the Van't Hoff Equation [6]. The expression $\Sigma_i \nu_i H_i(T)$ can be written as a function of temperature in terms of the heat capacity of the reacting species

$$\sum_i \nu_i H_i(T) = \sum_i \nu_i H_i^\circ(T^\circ) + \int_{T^\circ}^{T} \left(\sum_i \nu_i Cp_i(T)\right) dT \tag{15}$$

Values of $H_i^\circ(T^\circ)$ and $Cp_i^\circ(T^\circ)$ for different chemicals are available in the literature as tabulations of the standard Enthalpy of formation and the standard heat capacity. Assuming a constant $\Sigma_i \nu_i Cp_i(T)$ value, which equals $\Sigma_i \nu_i Cp_i^\circ(T^\circ)$

$$\sum_i \nu_i H_i(T) = \sum_i \nu_i H_i^\circ(T^\circ) + \left(T - T^\circ\right)\sum_i \nu_i Cp_i^\circ(T^\circ) \tag{16}$$

Substituting Equation (16) in (14)

$$R\frac{d\ln K}{dT} = \frac{\sum_i \nu_i H_i^\circ(T^\circ)}{T^2} + \sum_i \nu_i Cp_i^\circ(T^\circ)\left(\frac{1}{T} - \frac{T^\circ}{T^2}\right) \tag{17}$$

Integrating between T° and T gives

$$\ln K = \ln K^\circ - \frac{\sum_i \nu_i H_i^\circ(T^\circ)}{R}\left(\frac{1}{T} - \frac{1}{T^\circ}\right) - \frac{\sum_i \nu_i Cp_i^\circ(T^\circ)}{R}\left(\ln\frac{T^\circ}{T} - \frac{T^\circ}{T} + 1\right) \tag{18}$$

Where K° is given by

$$\ln K^\circ = \frac{-\sum_i \nu_i G_i^\circ(T^\circ)}{RT^\circ} \tag{19}$$

The reference state thermodynamic functions of the chemical reactions, ΔCp°, ΔH°, and ΔG°, are defined in terms of the reference state thermodynamic properties of the reacting species as follows

$$\Delta Cp^\circ = \sum_i \nu_i Cp_i^\circ \tag{20}$$

$$\Delta H^\circ = \sum_i \nu_i H_i^\circ \tag{21}$$

$$\Delta G^\circ = \sum_i \nu_i G_i^\circ \tag{22}$$

Equations (18) and (19) can now be rewritten using newly defined reference state thermodynamic functions of the chemical reactions as

$$\ln K = \ln K^\circ - \frac{\Delta H^\circ}{R}\left(\frac{1}{T} - \frac{1}{T^\circ}\right) - \frac{\Delta Cp^\circ}{R}\left(\ln\frac{T^\circ}{T} - \frac{T^\circ}{T} + 1\right) \tag{23}$$

$$\ln K^\circ = \frac{-\Delta G^\circ}{RT^\circ} \tag{24}$$

Equations (23) and (24) can be used to obtain the equilibrium constant of a chemical reaction as a function of temperature given the reference state thermodynamic properties of the reacting species.

A more accurate version of Equation (23) can be obtained by substituting a temperature-dependent heat capacity function, i.e. $Cp_i(T)$, in Equation (15), integrating it, and then proceeding with the same steps to get to Equation (23). Another alternative can be used to obtain a more accurate version of Equation (23) if experimental data of the equilibrium constant at various temperatures is available. ΔCp° and ΔH° can be used as adjustable parameters to fit the data to Equation (23) by means of non-linear regression. This will compensate for the temperature-independent heat capacity assumption used to develop that equation, which will result in better estimates of the equilibrium constants.

2.2 Ionic Activity

In 1887, Svanté Arrhenius [5] presented his theory of electrolytic dissociation of solute into negatively and positively charged ions. He assumed that the distribution and motion of ions in a solution is independent of the ionic interaction forces. Experimental work showed that Arrhenius' theory holds only for weak electrolytes, and that electrostatic forces between ions must be considered especially for strong electrolytes.

In 1923, Peter Debye and Erich Hückel [5] presented their theory of interionic attractions in electrolyte solutions. As electrolyte dissociation in solutions increases, ion concentration also increases resulting in smaller distance and greater electrostatic force between ions. The strength of this coulombic interaction between ions must therefore be considered in modeling thermodynamic equilibrium of electrolyte systems.

Ionic strength is a measure of the average electrostatic interactions among ions in an electrolyte. Lewis and Randall [1] defined the ionic strength as one-half the sum of the terms obtained by multiplying the molality of each ion by its valence squared

$$I = \frac{1}{2}\sum_i m_i z_i^2 \tag{25}$$

As previously mentioned, the chemical potential of species i in terms of its activity is

$$\mu_i(T) = \mu_i^\circ(T) + RT\ln(a_i) \tag{1}$$

Where the standard state is a hypothetical solution with molality m for which the activity coefficient is unity. The activity is related to molality by

$$a_i = \gamma_i m_i \tag{26}$$

Note that the activity can be related to other concentration scales, such as molarity and mole fraction scales. The units of activity are the same as those of the chosen concentration scale and the activity coefficient remains dimensionless always.

2.3 Ionic Activity Coefficient Models

Activity coefficient models for non-electrolyte binary and multi-component systems are available in the literature as Excess Gibbs Energy models. Different models handle different systems and one should be very careful when choosing a model to work with. Most of these models contain adjustable parameters that can be manipulated.

Debye-Hückel theory that was presented over seventy years ago provides the cornerstone for most models of electrolyte solutions. Classical Electrostatics and statistical mechanics are used to linearize the Poisson-Boltzmann distribution of charges, which will then approximate the ion-ion interaction energy allowing for the derivation of an expression for the mean ionic activity coefficient. Below are some ionic activity coefficient models for aqueous multi-component electrolyte solutions.

1. Debye-Hückel model [7]

$$-\log\gamma_i = \frac{Az_i^2\sqrt{I}}{1+\beta r_i\sqrt{I}} \tag{27}$$

Approximated values of r_i, the ion size parameter or the effective ionic radius, at 25 °C are given in Table 1 [7]. A and β are temperature-dependent parameters and can be estimated from the following polynomials that were obtained by fitting literature data found at temperatures between 0 and 100 °C [7]

$$A = (0.69725708) - (0.0021544338)T + (5.134952E-6)T^2 \tag{28}$$

$$\beta = (0.34905962) - (0.00032917649)T + (8.8002615E-7)T^2 \tag{29}$$

The Debye-Hückel model is satisfactory for weak electrolyte solutions of ionic strength of 0.1 molal or less but it gets progressively worse as ionic strength increases to practical engineering levels.

Table 1. Approximate Effective Ionic Radii in Aqueous Solutions at 25°C

r (Å)	*Inorganic Ions*	*r (Å)*	*Organic Ions*
2.5	Rb^+, Cs^+, NH_4^+, Tl^+, Ag^+	3.5	$HCOO^-$, H_2Cit^-, $CH_3NH_3^+$, $(CH_3)_2NH_2^+$
3	K^+, Cl^-, Br^-, I^-, CN^-, NO_2^-, NO_3^-	4	$H_3N^+CH_2COOH$, $(CH_3)_3NH^+$, $C_2H_5NH_3^+$
3.5	OH^-, F^-, SCN^-, OCN^-, HS^-, ClO_3^-, ClO_4^-, BrO_3^-, IO_4^-, MnO_4^-	4.5	CH_3COO^-, $ClCH_2COO^-$, $(CH_3)_4N^+$, $(C_2H_5)_2NH_2^+$, $H_2NCH_2COO^-$, oxalate^{2-}, $HCit^{2-}$
4	Na^+, $CdCl^+$, Hg_2^{2+}, ClO_2^-, IO_3^-, HCO_3^-, $H_2PO_4^-$, HSO_3^-, $H_2AsO_4^-$, SO_4^{2-}, $S_2O_3^{2-}$, $S_2O_8^{2-}$, SeO_4^{2-}, CrO_4^{2-}, HPO_4^{2-}, $S_2O_6^{2-}$, PO_4^{3-}, $Fe(CN)_6^{3-}$, $Cr(NH_3)_6^{3+}$, $Co(NH_3)_6^{3+}$, $Co(NH_3)_5H_2O^{3+}$	5	Cl_2CHCOO^-, Cl_3COO^-, $(C_2H_5)_3NH^+$, $C_3H_7NH_3^+$, Cit^{3-}, succinate^{2-}, malonate^{2-}, tartrate^{2-}
4.5	Pb^+, CO_3^{2-}, SO_3^{2-}, MoO_4^{2-}, $Co(NH_3)_5Cl^{2+}$, $Fe(CN)_5NO^{2-}$	6	benzoate$^-$, hydroxybenzoate$^-$, chlorobenzoate$^-$, phenylacetate$^-$, vinylacetate$^-$, $(CH_3)_2C{=}CHCOO^-$, $(C_2H_5)_4N^+$, $(C_3H_7)_2NH_2^+$, phthalate^{2-}, glutarate^{2-}, adipate^{2-}
5	Sr^{2+}, Ba^{2+}, Ra^{2+}, Cd^{2+}, Hg^{2+}, S^{2-}, $S_2O_4^{2-}$, WO_4^{2-}, $Fe(CN)_6^{4-}$	7	trinitrophenolate$^-$, $(C_3H_7)_3NH^+$, methoxybenzoate$^-$, pimelate^{2-}, suberate^{2-}, Congo red anion^{2-}
6	Li^+, Ca^{2+}, Cu^{2+}, Zn^{2+}, Sn^{2+}, Mn^{2+}, Fe^{2+}, Ni^{2+}, Co^{2+}, $Co(en)_3^{3+}$, $Co(S_2O_3)(CN)_5^{4-}$	8	$(C_6H_5)_2CHCOO^-$, $(C_3H_7)_4N^+$
8	Mg^{2+}, Be^{2+}		
9	H^+, Al^{3+}, Fe^{3+}, Cr^{3+}, Sc^{3+}, Y^{3+}, La^{3+}, In^{3+}, Ce^{3+}, Pr^{3+}, Nd^{3+}, Sm^{3+}, $Co(SO_3)_2(CN)_4^{5-}$		
11	Th^{4+}, Zr^{4+}, Ce^{4+}, Sn^{4+}		

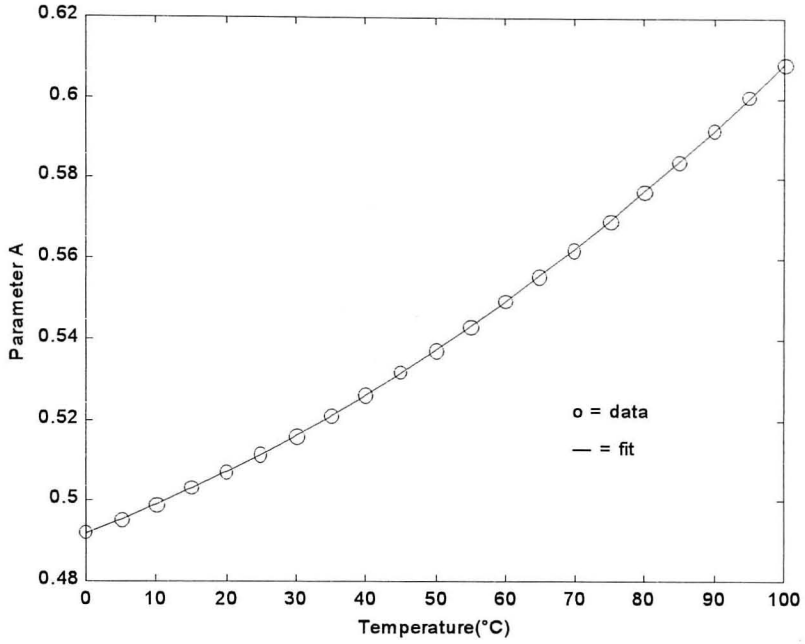

Figure 3. Debye-Hückel Parameter A as a Function of Temperature

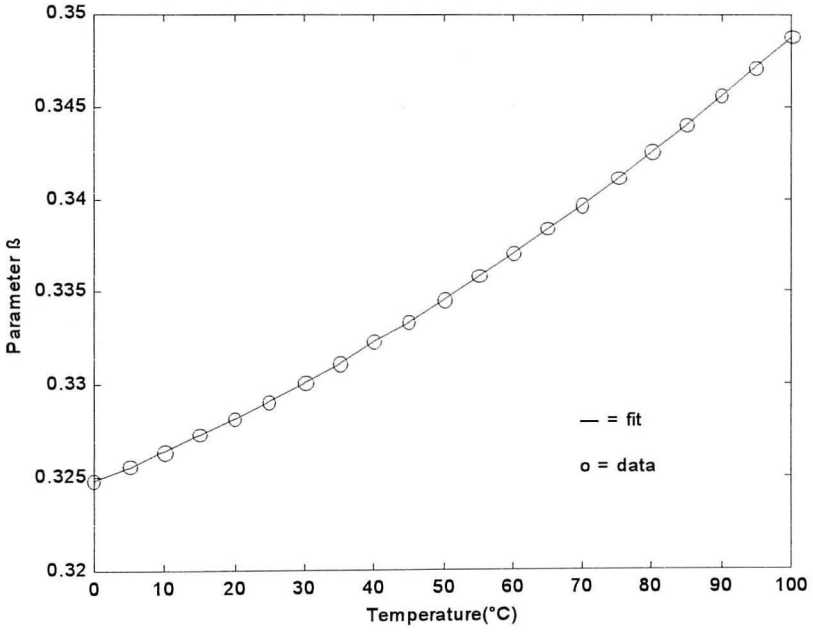

Figure 4. Debye-Hückel Parameter β as a Function of Temperature

2. Robinson-Guggenheim-Bates model [7]

$$-\log\gamma_i = \left(\frac{0.511I}{1+1.5I} - 0.2I\right)z_i^2 \tag{30}$$

The model is essentially a modified version of the Debye-Hückel model. The effective ionic radius is assumed to be 4.6 Å. This model is relatively successful for solutions up to 1 molal ionic strength and it is more convenient to implement than the Debye-Hückel model.

3. Bromley's model [5]

$$-\log\gamma_i = \frac{Az_i^2\sqrt{I}}{1+\sqrt{I}} - F_i \tag{31}$$

A is the Debye-Hückel parameter defined in Equation (28) and F_i is a summation of interaction parameters

$$F_i = \sum_j B_{ij}Z_{ij}^2 m_j \tag{32}$$

Where j can either indicate all anions in the solution if i were a cation, or all cations in the solution if i were an anion. Z_{ij} and B_{ij} are defined by

$$Z_{ij} = \frac{z_i + z_j}{2} \tag{33}$$

$$B_{ij} = \frac{(0.06+0.6B)\left|z_i z_j\right|}{\left(1+\frac{1.5I}{\left|z_i z_j\right|}\right)^2} + B \tag{34}$$

B is Bromley's parameter defined as

$$B = B^+ + B^- + \delta^+\delta^- \tag{35}$$

Values for B^+, B^-, δ^+, δ^- are available in Table 2 [5]. Bromley's model gives adequate results for strong electrolyte solutions up to ionic strengths of 6 molal.

Table 2. Bromley's Parameters for Different Electrolytes at 25°C

Cation	*B+*	*δ+*	*Anion*	*B-*	*δ-*
H^+	0.0875	0.103	F^-	0.0295	-0.930
Li^+	0.0691	0.138	Cl^-	0.0643	-0.067
Na^+	0.0000	0.028	Br^-	0.0741	0.064
K^+	-0.0452	-0.079	I^-	0.0890	0.196
Rb^+	-0.0537	-0.100	ClO_3^-	0.0050	0.450
Cs^+	-0.0710	-0.138	ClO_4^-	0.0020	0.790
NH_4^+	-0.0420	-0.020	BrO_3^-	-0.0320	0.140
Tl^+	-0.1350	-0.020	IO_3^-	-0.0400	0.000
Ag^+	-0.0580	0.000	NO_3^-	-0.0250	0.270
Be^{2+}	0.1000	0.200	$H_2PO_4^-$	-0.0520	0.200
Mg^{2+}	0.0570	0.157	$H_2AsO_4^-$	-0.0300	0.050
Ca^{2+}	0.0374	0.119	CNS^-	0.0710	0.160
Sr^{2+}	0.0245	0.110	OH^-	0.0760	-1.000
Ba^{2+}	0.0022	0.098	Formate	0.0720	-0.700
Mn^{2+}	0.0370	0.210	Acetate	0.1040	-0.730
Fe^{2+}	0.0460	0.210	Propionate	0.1520	-0.700
Co^{2+}	0.0490	0.210	Butyrate	0.1670	-0.700
Ni^{2+}	0.0540	0.210	Valerate	0.1420	-0.700
Cu^{2+}	0.0220	0.300	Caproate	0.0680	-0.700
Zn^{2+}	0.1010	0.090	Heptylate	-0.0270	-0.700
Cd^{2+}	0.0720	0.090	Caprylate	-0.1220	-0.700
Pb^{2+}	-0.1040	0.250	Pelargonate	-0.2840	-0.700
UO_2^{2+}	0.0790	0.190	Caprate	-0.4590	-0.700
Cr^{3+}	0.0660	0.150	H Malonate	0.0050	-0.220
Al^{3+}	0.0520	0.120	H Succinate	0.0210	-0.270
Sc^{3+}	0.0460	0.200	H Adipate	0.0530	-0.260
Y^{3+}	0.0370	0.200	Toluate	-0.0220	-0.160
La^{3+}	0.0360	0.270	CrO_4^{2-}	0.0190	-0.330
Ce^{3+}	0.0350	0.270	SO_4^{2-}	0.0000	-0.400
Pr^{3+}	0.0340	0.270	$S_2O_3^{2-}$	0.0190	-0.700
Nd^{3+}	0.0350	0.270	HPO_4^{2-}	-0.0100	-0.570
Sm^{3+}	0.0390	0.270	$HAsO_4^{2-}$	0.0210	-0.670
Eu^{3+}	0.0410	0.270	CO_3^{2-}	0.0280	-0.670
Ga^{3+}	0.0000	0.200	Fumarate	0.0560	-0.700
$Co(en)^{3+}$	-0.0890	0.000	Maleate	0.0170	-0.700
Th^{4+}	0.0620	0.190	PO_4^{3-}	0.0240	-0.700
			AsO_4^{3-}	0.0380	-0.780
			$Fe(CN)_6^{3-}$	0.0650	0.000
			$Mo(CN)_6^{3-}$	0.0560	0.000

Many other ionic activity coefficient models for electrolyte solutions are also available in the literature such as Guggenheim's Equation [5], Davies' Equation [5], Meissner's Equation [5], Pitzer's Equation [5], Chen's Equation [5], and National Bureau of Standards' Parametric Equations [5]. Most of these models predict the mean ionic activity coefficient of single and multi-component electrolyte solutions but not the ionic activity coefficient of individual ions.

2.4 Solid-Liquid Equilibria in Aqueous Solutions

Electrolytes dissolve in some solvents until they form a saturated solution of their constituent ions in equilibrium with the undissolved electrolytes. In a saturated solution, electrolytes continue to dissolve and an equal amount of ions in the solution keep combining to precipitate as a solid. Simple dissociation reactions can be represented as

$$C_m A_n(s) \underset{\text{Precipitation}}{\overset{\text{Dissolution}}{\longleftrightarrow}} mC^{c+}(aq) + nA^{a-}(aq)$$

The equilibrium constant for a dissolution reaction is called the solubility product, and is given by Equation (8). The solubility product of the given arbitrary dissolution reaction is

$$Ksp = \prod_i (a_i)^{\nu_i} = \frac{(a_C)^m (a_A)^n}{(a_{C_m A_n})} \tag{36}$$

The activity of the undissolved electrolytes or any other solid is obtained by

$$a_i = \gamma_i x_i \tag{37}$$

For slightly soluble electrolytes, deviation from ideality is minimum and the value of the activity coefficient approaches unity. Equation (36) can be rewritten as

$$Ksp = \frac{(a_C)^m (a_A)^n}{(x_{C_m A_n})} \tag{38}$$

Notice that *Ksp* at the standard conditions can be calculated by using the definition of the equilibrium constant given by Equation (7) or by using Van't Hoff's relationship [6] given by Equation (14).

2.5 Vapor-Liquid Equilibria in Aqueous Solutions

Some gases dissolve in electrolyte solutions and become in equilibrium with the undissolved gas. As before, this can be represented by

$$Kaq = \frac{a_i^L}{a_i^V} \tag{39}$$

a_i^L can be obtained using Equation (26), where a_i^V is related to the partial pressure of i by

$$a_i^V = f_i P_i \tag{40}$$

Notice that *Kaq* at the standard conditions can be calculated by using the definition of the equilibrium constant given by Equation (7) or by using Van't Hoff's relationship [6] given by Equation (14).

CHAPTER 3. THERMODYNAMIC MODEL OF PHOSPHATE LATTICE LOSS

3.1 Model Description

The large reactor used to extract phosphoric acid from phosphate rock in the dihydrate process contains the three distinct phases. The vapor phase can be safely considered an inert phase due to the low volatility of the reacting species and the small solubility of gases in the condensed phases. The liquid phase is mainly water along with phosphoric acid and small amounts of sulfuric acid. The solid phase is primarily gypsum with small quantity of phosphate present as dicalcium phosphate dihydrate or DCPD.

In a thermodynamic analysis, only major components and major reactions need to be considered. Trace components and reactions affect chemical kinetics but not to a great deal the thermodynamic equilibrium. The thermodynamic model of phosphate lattice loss mentioned earlier will be developed based upon the following equilibrium reactions

$$HSO_4^- \longleftrightarrow H^+ + SO_4^{2-}$$
$$H_3PO_4 \longleftrightarrow H^+ + H_2PO_4^-$$
$$H_2PO_4^- \longleftrightarrow H^+ + HPO_4^{2-}$$
$$CaHPO_4 \cdot 2H_2O \longleftrightarrow Ca^{2+} + HPO_4^{2-} + 2H_2O$$
$$CaSO_4 \cdot 2H_2O \longleftrightarrow Ca^{2+} + SO_4^{2-} + 2H_2O$$

Very slow chemical reactions, such as the dissolution of H_2O and HPO_4^{2-}, and very fast chemical reactions, such as the dissolution of H_2SO_4, do not disturb the equilibrium and thus will not be considered in the model.

3.2 Model Simulation

A thermodynamic model will be developed to predict the limits of distribution of phosphates between the liquid and the solid phases in the reactor used to extract phosphoric acid from phosphate rock. To track down the degrees of freedom, each equation in the model will be followed by a set of two numbers, a Roman number and an Arabic number, that will work as a counter. The first number will count the number of equations while the second number will count the number of unknowns and the difference between the two numbers is the degree of freedom of the model.

Defining the liquid phase properties: total phosphate molality (*TPM*) and total sulfate molality (*TSM*)

$$TPM = m_{H_3PO_4} + m_{H_2PO_4^-} + m_{HPO_4^{2-}} \qquad \text{(i, 4)}$$

$$TSM = m_{HSO_4^-} + m_{SO_4^{2-}} \qquad \text{(ii, 7)}$$

The total phosphates content of the liquid phase is a known parameter and can be expressed as percent P_2O_5 equivalence by mass (Kg P_2O_5 / Kg Solution)

$$\%P_2O_5 = \left(TPM \times \Theta_{P_2O_5} \times MW_{P_2O_5} \times \Phi_{H_2O}\right) \times 100 \qquad \text{(iii, 8)}$$

The effective sulfuric acid content of the liquid phase is a manipulated parameter and can be expressed as percent H_2SO_4 equivalence by mass (Kg H_2SO_4 / Kg Solution)

$$\%H_2SO_4 = \left(TSM \times \Theta_{H_2SO_4} \times MW_{H_2SO_4} \times \Phi_{H_2O}\right) \times 100 \qquad \text{(iv, 8)}$$

$\%P_2O_5$ is taken to be 28% mass, while $\%H_2SO_4$ will be varied to study its effect on the distribution of phosphates. The variable Θ_i indicates the moles of species i equivalence per 1 mole of its prospective compounds; therefore, Θ_{P2O5} is equal to ½ and Θ_{H2SO4} is equal to 1.

The variable Φ_{H2O} is the mass fraction of water in the liquid

$$\Phi_{H_2O} = M_{H_2O} / M_{Total} \qquad \text{(v, 9)}$$

The variable M_i represents the total mass of i in the liquid per total mass of water in the liquid. This corresponds to a value of unity for M_{H2O} and a value that is greater than unity for M_{Total}.

The molality of water is a fixed value and will be used later in the model. It is defined as the inverse of the molecular weight of water

$$m_{H_2O} = 1 / MW_{H_2O} \qquad \text{(vi, 10)}$$

Conducting a total mass balance in the liquid phase for total phosphate molality and total sulfate molality

$$M_{TPM} = (m_{H_3PO_4} \times MW_{H_3PO_4}) + (m_{H_2PO_4^-} \times MW_{H_2PO_4^-}) + (m_{HPO_4^{2-}} \times MW_{HPO_4^{2-}}) \qquad \text{(vii, 11)}$$

$$M_{TSM} = (m_{HSO_4^-} \times MW_{HSO_4^-}) + (m_{SO_4^{2-}} \times MW_{SO_4^-}) \qquad \text{(viii, 12)}$$

Total mass balance for the remaining species, e. g. Ca^{2+} and H^+, in the liquid phase

$$M_{Other} = (m_{H^+} \times MW_{H^+}) + (m_{Ca^{2+}} \times MW_{Ca^{2+}}) \qquad \text{(ix, 15)}$$

An overall mass balance can be written as

$$M_{Total} = M_{H_2O} + M_{TPM} + M_{TSM} + M_{Other} \qquad \text{(x, 15)}$$

A charge balance is needed to satisfy the electroneutrality condition

$$z_{H_2PO_4^-} m_{H_2PO_4^-} + z_{HPO_4^{2-}} m_{HPO_4^{2-}} + z_{HSO_4^-} m_{HSO_4^-} + z_{SO_4^{2-}} m_{SO_4^{2-}} + z_{H^+} m_{H^+} + z_{Ca^{2+}} m_{Ca^{2+}} = 0$$

(xi, 15)

The liquid phase acid equilibria are included in the model by the equilibrium relations. The equilibrium relations for the dissolution of HSO_4^-, H_3PO_4, and $H_2PO_4^-$ are expressed in terms of species activities as follows

$$K_{HSO_4^-} = \frac{a_{SO_4^{2-}} \times a_{H^+}}{a_{HSO_4^-}} \qquad \text{(xii, 19)}$$

$$K_{H_3PO_4} = \frac{a_{H_2PO_4^-} \times a_{H^+}}{a_{H_3PO_4}} \qquad \text{(xiii, 22)}$$

$$K_{H_2PO_4^-} = \frac{a_{HPO_4^{2-}} \times a_{H^+}}{a_{H_2PO_4^-}} \qquad \text{(xiv, 24)}$$

The solid-liquid equilibria are included in the model by the solubility product relations. The solubility product relations for gypsum and DCPD are

$$Ksp_{Gypsum} = \frac{a_{SO_4^{2-}} \times a_{Ca^{2+}} \times a_{H_2O}{}^2}{x_{Gypsum}} \qquad \text{(xv, 28)}$$

$$Ksp_{DCPD} = \frac{a_{HPO_4^{2-}} \times a_{Ca^{2+}} \times a_{H_2O}{}^2}{x_{DCPD}} \qquad \text{(xvi, 30)}$$

Neglecting the presence of impurities and assuming that the solid phase consists of only gypsum and DCPD

$$x_{Gypsum} + x_{DCPD} = 1 \qquad \text{(xvii, 30)}$$

Mass fraction of DCPD in the solid solution can be obtained by

$$\omega_{DCPD} = \frac{\left(x_{Gypsum} \times MW_{Gypsum}\right)}{\left(x_{Gypsum} \times MW_{Gypsum} + x_{DCPD} \times MW_{DCPD}\right)} \qquad \text{(xviii, 31)}$$

The phosphate lattice loss, $\%P_2O_5{}^{(S)}$, can be expressed as percent P_2O_5 equivalence by mass (Kg P_2O_5 / Kg Solid)

$$\%P_2O_5{}^{(S)} = \left(\omega_{DCPD} \times \left(\frac{1}{MW_{DCPD}}\right) \times \Psi_{P_2O_5} \times MW_{P_2O_5}\right) \times 100 \qquad \text{(xix, 32)}$$

The variable Ψ_{P2O5} is defined in a similar way to the variable Θ_{P2O5}. It indicates the moles of P_2O_5 equivalence per 1 mole of DCPD; therefore, Ψ_{P2O5} is equal to ½.

Temperature-dependent equilibrium constants of the model reactions can be captured using Equation (23) developed in Chapter 2

$$\ln K_{HSO_4^-} = \ln K^\circ_{HSO_4^-} - \frac{\Delta H^\circ_{HSO_4^-}}{R}\left(\frac{1}{T} - \frac{1}{T^\circ}\right) - \frac{\Delta Cp^\circ_{HSO_4^-}}{R}\left(\ln\frac{T^\circ}{T} - \frac{T^\circ}{T} + 1\right) \quad \text{(xx, 35)}$$

$$\ln K_{H_3PO_4} = \ln K^\circ_{H_3PO_4} - \frac{\Delta H^\circ_{H_3PO_4}}{R}\left(\frac{1}{T} - \frac{1}{T^\circ}\right) - \frac{\Delta Cp^\circ_{H_3PO_4}}{R}\left(\ln\frac{T^\circ}{T} - \frac{T^\circ}{T} + 1\right) \quad \text{(xxi, 38)}$$

$$\ln K_{H_2PO_4^-} = \ln K^\circ_{H_2PO_4^-} - \frac{\Delta H^\circ_{H_2PO_4^-}}{R}\left(\frac{1}{T} - \frac{1}{T^\circ}\right) - \frac{\Delta Cp^\circ_{H_2PO_4^-}}{R}\left(\ln\frac{T^\circ}{T} - \frac{T^\circ}{T} + 1\right) \quad \text{(xxii, 41)}$$

$$\ln K_{Gypsum} = \ln K^\circ_{Gypsum} - \frac{\Delta H^\circ_{Gypsum}}{R}\left(\frac{1}{T} - \frac{1}{T^\circ}\right) - \frac{\Delta Cp^\circ_{Gypsum}}{R}\left(\ln\frac{T^\circ}{T} - \frac{T^\circ}{T} + 1\right) \quad \text{(xxiii, 44)}$$

$$\ln K_{DCPD} = \ln K^\circ_{DCPD} - \frac{\Delta H^\circ_{DCPD}}{R}\left(\frac{1}{T} - \frac{1}{T^\circ}\right) - \frac{\Delta Cp^\circ_{DCPD}}{R}\left(\ln\frac{T^\circ}{T} - \frac{T^\circ}{T} + 1\right) \quad \text{(xxiv, 47)}$$

Temperature of the medium is a manipulated parameter that will be varied to study its effect on the distribution of phosphates. The reference state equilibrium constants can be obtained using Equation (24) defined in Chapter 2

$$\ln K^\circ_{HSO_4^-} = \frac{-\Delta G^\circ_{HSO_4^-}}{RT^\circ} \quad \text{(xxv, 48)}$$

$$\ln K^\circ_{H_3PO_4} = \frac{-\Delta G^\circ_{H_3PO_4}}{RT^\circ} \quad \text{(xxvi, 49)}$$

$$\ln K^\circ_{H_2PO_4^-} = \frac{-\Delta G^\circ_{H_2PO_4^-}}{RT^\circ} \quad \text{(xxvii, 50)}$$

$$\ln K^\circ_{Gypsum} = \frac{-\Delta G^\circ_{Gypsum}}{RT^\circ} \quad \text{(xxviii, 51)}$$

$$\ln K^\circ_{DCPD} = \frac{-\Delta G^\circ_{DCPD}}{RT^\circ} \quad \text{(xxix, 52)}$$

The reference state thermodynamic functions of the model reactions, ΔCp°, ΔH°, and ΔG°, can be easily computed using the reference state thermodynamic properties of the reacting species available in the literature. ΔCp° expressions for this model are defined as follows

$$\Delta Cp^{\circ}_{HSO_4^-} = \sum_i \nu_i Cp^{\circ}_i = Cp^{\circ}_{SO_4^{2-}} + Cp^{\circ}_{H^+} - Cp^{\circ}_{HSO_4^-} \quad \text{(xxx, 52)}$$

$$\Delta Cp^{\circ}_{H_3PO_4} = \sum_i \nu_i Cp^{\circ}_i = Cp^{\circ}_{H_2PO_4^-} + Cp^{\circ}_{H^+} - Cp^{\circ}_{H_3PO_4} \quad \text{(xxxi, 52)}$$

$$\Delta Cp^{\circ}_{H_2PO_4^-} = \sum_i \nu_i Cp^{\circ}_i = Cp^{\circ}_{HPO_4^{2-}} + Cp^{\circ}_{H^+} - Cp^{\circ}_{H_2PO_4^-} \quad \text{(xxxii, 52)}$$

$$\Delta Cp^{\circ}_{Gypsum} = \sum_i \nu_i Cp^{\circ}_i = Cp^{\circ}_{Ca^{2+}} + Cp^{\circ}_{SO_4^{2-}} + 2 \times Cp^{\circ}_{H_2O} - Cp^{\circ}_{Gypsum} \quad \text{(xxxiii, 52)}$$

$$\Delta Cp^{\circ}_{DCPD} = \sum_i \nu_i Cp^{\circ}_i = Cp^{\circ}_{Ca^{2+}} + Cp^{\circ}_{HPO_4^{2-}} + 2 \times Cp^{\circ}_{H_2O} - Cp^{\circ}_{DCPD} \quad \text{(xxxiv, 52)}$$

Similarly, ΔH° expressions for this model are

$$\Delta H^{\circ}_{HSO_4^-} = \sum_i \nu_i H^{\circ}_i = H^{\circ}_{SO_4^{2-}} + H^{\circ}_{H^+} - H^{\circ}_{HSO_4^-} \quad \text{(xxxv, 52)}$$

$$\Delta H^{\circ}_{H_3PO_4} = \sum_i \nu_i H^{\circ}_i = H^{\circ}_{H_2PO_4^-} + H^{\circ}_{H^+} - H^{\circ}_{H_3PO_4} \quad \text{(xxxvi, 52)}$$

$$\Delta H^{\circ}_{H_2PO_4^-} = \sum_i \nu_i H^{\circ}_i = H^{\circ}_{HPO_4^{2-}} + H^{\circ}_{H^+} - H^{\circ}_{H_2PO_4^-} \quad \text{(xxxvii, 52)}$$

$$\Delta H^{\circ}_{Gypsum} = \sum_i \nu_i H^{\circ}_i = H^{\circ}_{Ca^{2+}} + H^{\circ}_{SO_4^{2-}} + 2 \times H^{\circ}_{H_2O} - H^{\circ}_{Gypsum} \quad \text{(xxxviii, 52)}$$

$$\Delta H^{\circ}_{DCPD} = \sum_i \nu_i H^{\circ}_i = H^{\circ}_{Ca^{2+}} + H^{\circ}_{HPO_4^{2-}} + 2 \times H^{\circ}_{H_2O} - H^{\circ}_{DCPD} \quad \text{(xxxix, 52)}$$

If experimental data of the equilibrium constant at various temperatures is available, ΔCp° and ΔH° can be used as adjustable parameters to fit the data to Equation (23) by means of non-linear regression. This will compensate for the temperature-independent heat capacity assumption used to develop that equation, which will result in better estimates of the temperature-dependent equilibrium constants.

Likewise, ΔG° expressions for this model are

$$\Delta G^{\circ}_{HSO_4^-} = \sum_i \nu_i G_i^{\circ} = G^{\circ}_{SO_4^{2-}} + G^{\circ}_{H^+} - G^{\circ}_{HSO_4^-} \quad \text{(xxxx, 52)}$$

$$\Delta G^{\circ}_{H_3PO_4} = \sum_i \nu_i G_i^{\circ} = G^{\circ}_{H_2PO_4^-} + G^{\circ}_{H^+} - G^{\circ}_{H_3PO_4} \quad \text{(xxxxi, 52)}$$

$$\Delta G^{\circ}_{H_2PO_4^-} = \sum_i \nu_i G_i^{\circ} = G^{\circ}_{HPO_4^{2-}} + G^{\circ}_{H^+} - G^{\circ}_{H_2PO_4^-} \quad \text{(xxxxii, 52)}$$

$$\Delta G^{\circ}_{Gypsum} = \sum_i \nu_i G_i^{\circ} = G^{\circ}_{Ca^{2+}} + G^{\circ}_{SO_4^{2-}} + 2 \times G^{\circ}_{H_2O} - G^{\circ}_{Gypsum} \quad \text{(xxxxiii, 52)}$$

$$\Delta G^{\circ}_{DCPD} = \sum_i \nu_i G_i^{\circ} = G^{\circ}_{Ca^{2+}} + G^{\circ}_{HPO_4^{2-}} + 2 \times G^{\circ}_{H_2O} - G^{\circ}_{DCPD} \quad \text{(xxxxiv, 52)}$$

Equation (26) gives the definition of activity and how it is related to molality by the activity coefficient. Expanding Equation (26) to define the activities of the reacting species

$$a_{H_2O} = \gamma_{H_2O} \times m_{H_2O} \quad \text{(xxxxv, 53)}$$

$$a_{H_3PO_4} = \gamma_{H_3PO_4} \times m_{H_3PO_4} \quad \text{(xxxxvi, 54)}$$

$$a_{H_2PO_4^-} = \gamma_{H_2PO_4^-} \times m_{H_2PO_4^-} \quad \text{(xxxxvii, 55)}$$

$$a_{HPO_4^{2-}} = \gamma_{HPO_4^{2-}} \times m_{HPO_4^{2-}} \quad \text{(xxxxviii, 56)}$$

$$a_{HSO_4^-} = \gamma_{HSO_4^-} \times m_{HSO_4^-} \quad \text{(xxxxix, 57)}$$

$$a_{SO_4^{2-}} = \gamma_{SO_4^{2-}} \times m_{SO_4^{2-}} \quad \text{(xxxxx, 58)}$$

$$a_{H^+} = \gamma_{H^+} \times m_{H^+} \quad \text{(xxxxxi, 59)}$$

$$a_{Ca^{2+}} = \gamma_{Ca^{2+}} \times m_{Ca^{2+}} \quad \text{(xxxxxii, 60)}$$

The degree of freedom of the model is now 8 and it needs to be brought down to zero to run the simulation. The last set of equations contains eight activity coefficients that are not yet defined.

Before defining those activity coefficients, an expression for the ionic strength of the aqueous solution is needed. Using Equation (25), the ionic strength of the solution can be written as

$$I = \frac{1}{2}\left[\begin{array}{l}\left(m_{H_2PO_4^-} \times z^2_{H_2PO_4^-}\right)+\left(m_{HPO_4^{2-}} \times z^2_{HPO_4^{2-}}\right)+\left(m_{HSO_4^-} \times z^2_{HSO_4^-}\right)\\ +\left(m_{SO_4^{2-}} \times z^2_{SO_4^{2-}}\right)+\left(m_{H^+} \times z^2_{H^+}\right)+\left(m_{Ca^{2+}} \times z^2_{Ca^{2+}}\right)\end{array}\right] \qquad \text{(xxxxxiii, 61)}$$

The hydrogen ion activity in a solution is an important concept in many chemical and biological processes. The magnitude of this activity is measured by the *pH*, where

$$pH = -\log_{10}\left(a_{H^+} \times \rho_{H_2O}\right) \qquad \text{(xxxxxiv, 62)}$$

Note that the mass density of water was used to convert the activity concentration scale from molality to molarity as required by the *pH* definition. In other words, *pH* is the negative base 10-logarithm of the hydrogen ion activity given by molarity units.

Finally, activity coefficients of the reacting species must be defined to bring this model to completion. The following correlations [14] for the activity coefficients of phosphoric acid and water were determined from vapor pressure data of pure solutions of phosphoric acid and water at 25 °C and they will be used in the simulation

$$\gamma_{H_2O} = -(0.87979) + (0.75533)\%P_2O_5 - (0.0012084)\%P_2O_5{}^2 + \frac{(15.258)}{\%P_2O_5} \qquad \text{(xxxxxv, 62)}$$

$$\gamma_{H_3PO_4} = (22.676) - (1.0192)\%P_2O_5 + (0.01891)\%P_2O_5{}^2 - \frac{(159.56)}{\%P_2O_5} \qquad \text{(xxxxxvi, 62)}$$

Three sets of electrolyte activity coefficients will be employed to complete the model. Ideal solution, Debye-Hückel, and Robinson-Guggenheim-Bates models [7] will be used alternately to write the activity coefficients of the remaining electrolytes. The simulation will be carried out utilizing each model and the three outputs will then be compared to one another.

Ideal solution model assumes that the physical properties of the mixture are not influenced by temperature or concentration and that there are no interactions between components; therefore, in an ideal solution, the activity of a substance is equal to its concentration. This corresponds to activity coefficients that equal unity

$$\gamma_{H_2PO_4^-} = \gamma_{HPO_4^{2-}} = \gamma_{HSO_4^-} = \gamma_{SO_4^{2-}} = \gamma_{H^+} = \gamma_{Ca^{2+}} = 1 \qquad \text{(xxxxxviia-xxxxxxiia, 62)}$$

The ideal solution model provides a limiting case for the behavior of an actual solution. The model can describe real solutions at low concentrations.

In 1923 and for the first time, ion-ion and ion-solvent interactions were accounted for in an electrolyte model proposed by Debye and Hückel. The Debye-Hückel model also accounts for temperature and ionic radius effects on solution behavior. Activity coefficients based on this model are obtained using Equation (27)

$$-\log\gamma_{H_2PO_4^-} = \frac{Az^2_{H_2PO_4^-}\sqrt{I}}{1+\beta r_{H_2PO_4^-}\sqrt{I}} \qquad \text{(xxxxxviib, 62)}$$

$$-\log\gamma_{HPO_4^{2-}} = \frac{Az^2_{HPO_4^{2-}}\sqrt{I}}{1+\beta r_{HPO_4^{2-}}\sqrt{I}} \qquad \text{(xxxxxviiib, 62)}$$

$$-\log\gamma_{HSO_4^-} = \frac{Az^2_{HSO_4^-}\sqrt{I}}{1+\beta r_{HSO_4^-}\sqrt{I}} \qquad \text{(xxxxxixb, 62)}$$

$$-\log\gamma_{SO_4^{2-}} = \frac{Az^2_{SO_4^{2-}}\sqrt{I}}{1+\beta r_{SO_4^{2-}}\sqrt{I}} \qquad \text{(xxxxxxb, 62)}$$

$$-\log\gamma_{H^+} = \frac{Az^2_{H^+}\sqrt{I}}{1+\beta r_{H^+}\sqrt{I}} \qquad \text{(xxxxxxib, 62)}$$

$$-\log\gamma_{Ca^{2+}} = \frac{Az^2_{Ca^{2+}}\sqrt{I}}{1+\beta r_{Ca^{2+}}\sqrt{I}} \qquad \text{(xxxxxxiib, 62)}$$

Values of r_i, A, and β are available in the literature. Values of r_i for many common electrolytes are given in Table 1 [7] while Equations (28) and (29) provide estimates for A and β as functions of temperature. The Debye-Hückel model generates adequate results for weak electrolyte solutions up to 0.1 molal ionic strength.

The third set of electrolyte activity coefficients that will be used is given by the Robinson-Guggenheim-Bates model. The model adds a considerable improvement to the Debye-Hückel model by subtracting an adjustable parameter term that will increase the range of adequacy up to 1 molal ionic strength. Activity coefficients based on this model are obtained using Equation (30)

$$-\log\gamma_{H_2PO_4^-} = \left(\frac{0.511\sqrt{I}}{1+1.5I} - 0.2I\right) z^2_{H_2PO_4^-} \qquad \text{(xxxxxviic, 62)}$$

$$-\log\gamma_{HPO_4^{2-}} = \left(\frac{0.511\sqrt{I}}{1+1.5I} - 0.2I\right) z^2_{HPO_4^{2-}} \qquad \text{(xxxxxviiic, 62)}$$

$$-\log\gamma_{HSO_4^-} = \left(\frac{0.511\sqrt{I}}{1+1.5I} - 0.2I\right) z^2_{HSO_4^-} \qquad \text{(xxxxxixc, 62)}$$

$$-\log\gamma_{SO_4^{2-}} = \left(\frac{0.511\sqrt{I}}{1+1.5I} - 0.2I\right) z^2_{SO_4^{2-}} \qquad \text{(xxxxxxc, 62)}$$

$$-\log\gamma_{H^+} = \left(\frac{0.511\sqrt{I}}{1+1.5I} - 0.2I\right) z^2_{H^+} \qquad \text{(xxxxxxic, 62)}$$

$$-\log\gamma_{Ca^{2+}} = \left(\frac{0.511\sqrt{I}}{1+1.5I} - 0.2I\right) z^2_{Ca^{2+}} \qquad \text{(xxxxxxiic, 62)}$$

The model is now complete with 62 unknowns to solve using 62 equations. A computer code will be used to solve the model using different inputs of temperatures, liquid phase sulfuric acid contents, and electrolyte activity coefficient models.

CHAPTER 4. RESULTS AND DISCUSSION

4.1 Temperature Effect on Equilibrium

Experimental data of equilibrium constants [7] and solubility products [8] [9] [10] of model reactions were found at various temperatures. Least squares regression was used to fit the data points to Equation (23) by manipulating the values of ΔCp° and ΔH°.

$$\ln K = \ln K^\circ - \frac{\Delta H^\circ}{R}\left(\frac{1}{T} - \frac{1}{T^\circ}\right) - \frac{\Delta Cp^\circ}{R}\left(\ln\frac{T^\circ}{T} - \frac{T^\circ}{T} + 1\right) \qquad (23)$$

Table 3 displays two values of ΔCp° and ΔH° for each equilibrium reaction. One of those two values is the stoichiometric sum of the reference state thermodynamic properties of the reacting species found in the literature [7] [11] [12] [13]. The other value is the adjusted value by least squares regression to fit the data points to Equation (23).

Table 3. Literature and Regressed Values of Thermodynamic Functions

Equilibrium Reaction	ΔCp° (J/mol K)		ΔH° (J/mol)	
	literature	regression	literature	regression
$HSO_4^- \longleftrightarrow H^+ + SO_4^{2-}$	-209.00	-310.01	-21930	-16928
$H_3PO_4 \longleftrightarrow H^+ + H_2PO_4^-$	-155.00	-155.41	-7950	-7663
$H_2PO_4^- \longleftrightarrow H^+ + HPO_4^{2-}$	-226.00	-248.97	+4150	+4034
$CaSO_4 \cdot 2H_2O \longleftrightarrow Ca^{2+} + SO_4^{2-} + 2H_2O$	-365.30	-493.59	-1160	+4338
$CaHPO_4 \cdot 2H_2O \longleftrightarrow Ca^{2+} + HPO_4^{2-} + 2H_2O$	-399.30	-878.73	-3050	-3050

Equation 23 was developed assuming a temperature-independent heat capacity to simplify the integration of the heat capacity function; therefore, the difference between the two values of ΔCp° and ΔH° for each reaction given in Table 3 shows the magnitude of heat capacity dependence on temperature. The closer the adjusted values to the reference state values of ΔCp° and ΔH° are, the more independent from temperature heat capacity is likely to be and vice versa. It is noteworthy to mention that the two values of ΔCp° and ΔH° for each reaction given in Table 3 are presented to show the degree of heat capacity dependence on temperature and not to compare both values to one another.

The heat capacity of dissolution for H_3PO_4 is almost independent of temperature, while for $H_2PO_4^-$ is slightly dependent on temperature. On the other hand, the heat capacity of dissolution for HSO_4^- is most likely a strong function of temperature. The heat capacity of solubility for gypsum is probably dependent on temperature to a great extent. The adjusted $\Delta H_{Gypsum}^{\circ}$ value was considerably different from the reference state value of $\Delta H_{Gypsum}^{\circ}$ in order to account for that dependence. Only two data points of DCPD solubility product [9] [10] were found and used in the regression. The reference state value of ΔH_{DCPD}° was kept the same and ΔCp_{DCPD}° was adjusted to fit a straight line through the two data points. The heat capacity of solubility for DCPD seems to have significant temperature dependence.

Temperature effect on equilibrium and the results of Table 3 can be illustrated by Figures 5 through 9. Equilibrium constants and solubility products were computed and plotted versus temperature using both values of ΔCp° and ΔH° given in Table 3. Experimental data were also plotted with both computed values to show the degree of accuracy or the degree of deviation of the computed values.

The adjusted values of ΔCp° and ΔH° were used in the simulation rather than the reference state values because they give a more accurate representation of the thermodynamic equilibrium as demonstrated by Figures 5 through 9. However, If calculations are to be carried out at the reference state temperature of 25 °C, Equation (23) reduces to Equation (24) and the values of ΔCp° and ΔH° become irrelevant. Equation (24) was developed earlier in chapter two and is given by

$$\ln K^{\circ} = \frac{-\Delta G^{\circ}}{RT^{\circ}} \tag{24}$$

Generally, ΔCp° and ΔH° for any constant temperature simulation become insignificant provided that the equilibrium constants or the partial molar Gibbs free energy for the different species are available at that temperature.

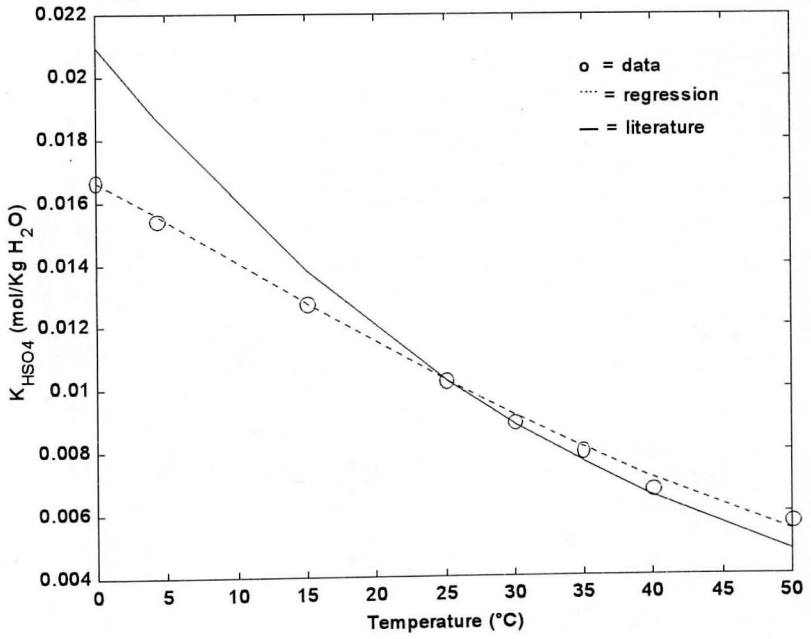

Figure 5. K_{HSO4} as a Function of Temperature

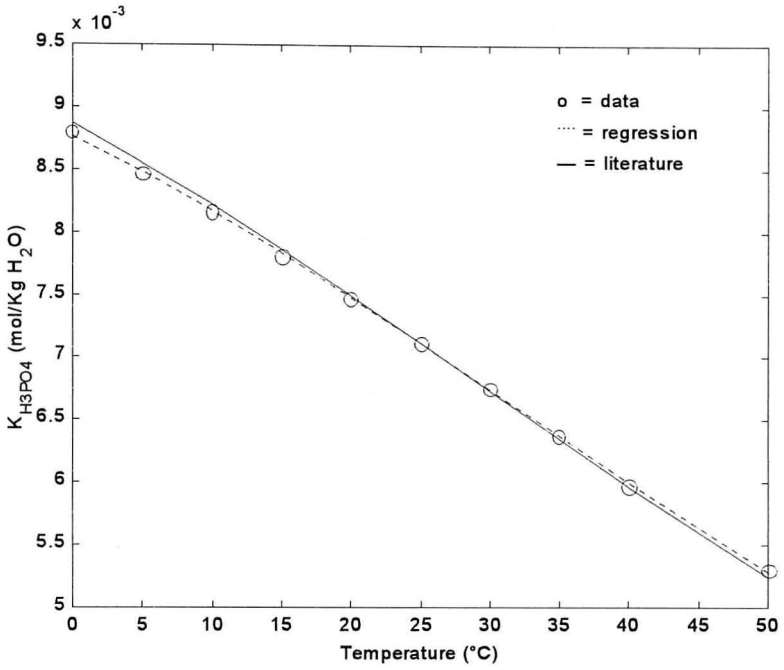

Figure 6. K_{H3PO4} as a Function of Temperature

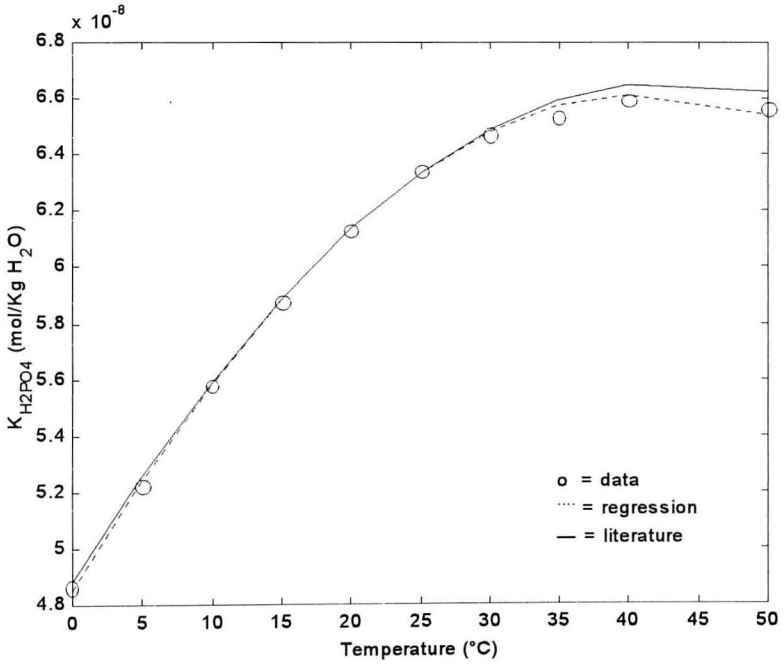

Figure 7. K_{H2PO4} as a Function of Temperature

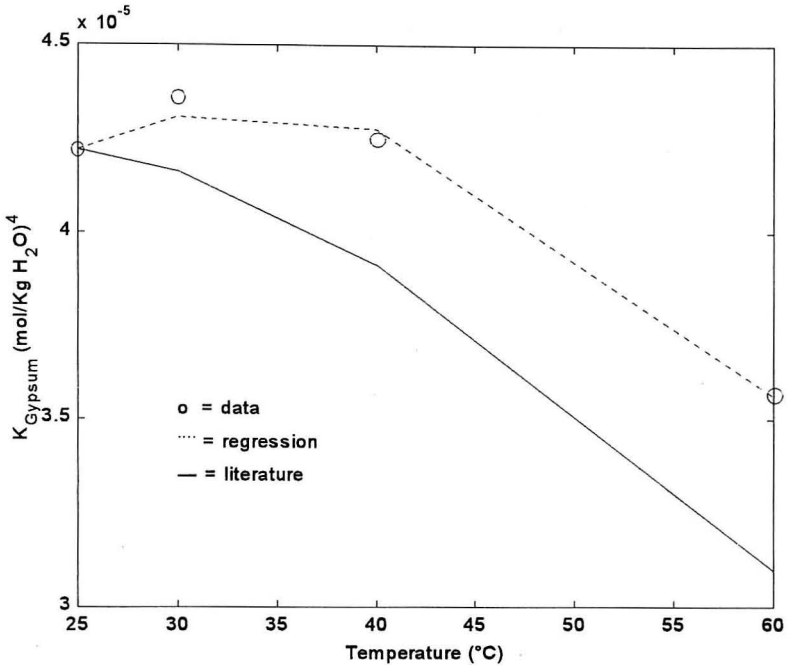

Figure 8. K_{Gypsum} as a Function of Temperature

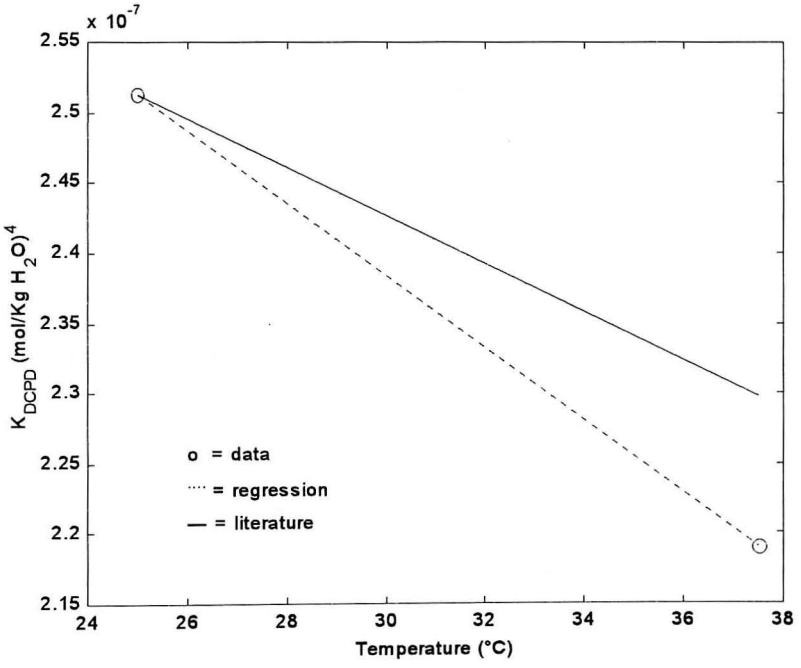

Figure 9. K_{DCPD} as a Function of Temperature

4.2 Temperature Effect on System Variables

Using temperature as an input list that varied from 0 to 100 °C, the simulation was ran using three different activity coefficient models: ideal solution, Debye-Hückel, and Robinson-Guggenheim-Bates. Each simulation run was carried out with five different inputs of the effective sulfuric acid content of the liquid phase.

Ionic strength decreased linearly with increasing temperature. This result shows that the average degree of ionization, and thus the electrostatic interactions among ions, tends to decrease with increasing temperature. The ideal solution model predicted the lowest values for ionic strength while the Debye-Hückel model predicted the highest. Robinson-Guggenheim-Bates model predicted intermediate values for ionic strength but closer to those predicted by the ideal solution model. Furthermore, Debye-Hückel and Robinson-Guggenheim-Bates models prediction of ionic strength becomes closer to the ideal solution model prediction as ionic strength value decreases. This is expected since both models reduce to the ideal solution model at an ionic strength of zero.

The liquid phase *pH* increased almost linearly with increasing temperature. This result shows that the activity, and thus the molality, of the hydrogen ion tends to decrease with increasing temperature. This observation is in agreement with the previous one concerning ionic strength. As temperature increases, the average degree of ionization decreases which will decrease the molality and activity of the hydrogen ion. For most of the temperature range, the ideal solution model predicted the lowest values while the Robinson-Guggenheim-Bates model predicted the highest. The Debye-Hückel model on the other hand, predicted intermediate *pH* values for temperatures between 20 and 70 °C, lowest for temperatures below 20 °C, and highest for temperatures above 70 °C.

The solid phase content of DCPD expressed as % P_2O_5, also known as the phosphate lattice loss, is the variable of most interest. Simulation results indicated that phosphate lattice loss increased rapidly with increase in temperature. As was shown earlier, the solubility product of DCPD decreases as temperature increases, which is in agreement with increasing phosphate losses at elevated temperatures.

The ideal solution model predicted the lowest values for phosphate lattice loss while the Debye-Hückel model predicted the highest. Robinson-Guggenheim-Bates model predicted intermediate values for phosphate lattice loss but closer to those predicted by the ideal solution model. Furthermore, Debye-Hückel and Robinson-Guggenheim-Bates models prediction of phosphate lattice loss becomes closer to the ideal solution model prediction as temperature decreases.

According to the Equilibrium constants and the solubility products plots, low reactor temperatures will increase the dissolution of DCPD and decrease the dissolution of gypsum. This will increase the solid content of gypsum and decrease its content of DCPD. Low reactor temperatures will also increase the dissociation of HSO_4^-, which will increase the concentration of SO_4^{2-} ions in the aqueous solution. This will shift the equilibrium of gypsum towards more precipitation. On the contrary, low reactor temperatures will decrease the dissociation of $H_2PO_4^-$, which will decrease the concentration of HPO_4^{2-} ions in the aqueous solution. This will shift the equilibrium of DCPD towards more dissolution.

Before deciding on how low of a temperature the reactor should be operated at, more equilibrium data is needed to perform more meticulous regression and obtain more precise values of the equilibrium constants especially for gypsum and DCPD.

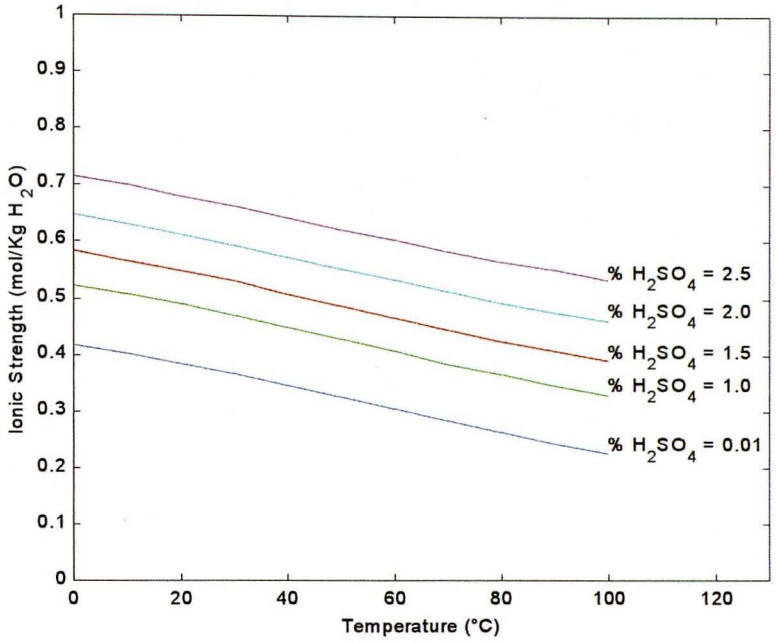

Figure 10. Ionic Strength Versus Temperature – Ideal Solution Model

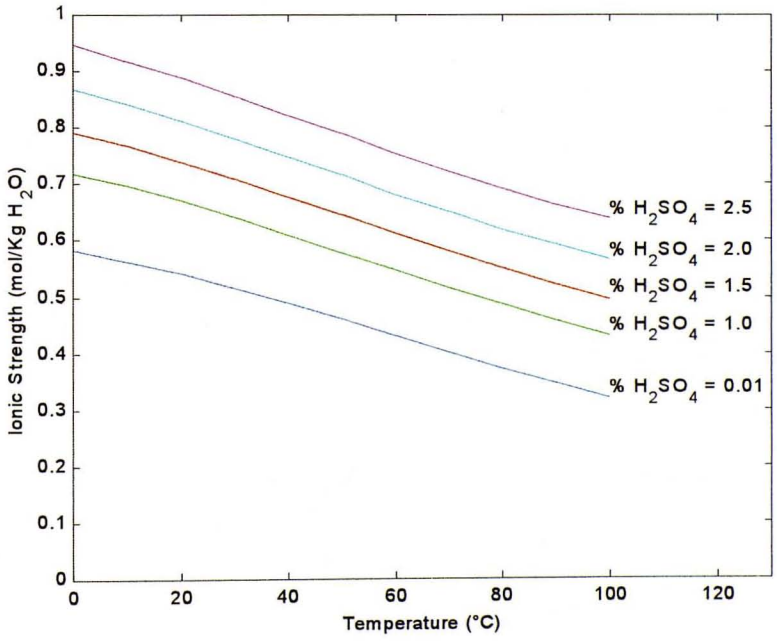

Figure 11. Ionic Strength Versus Temperature – Debye-Hückel Model

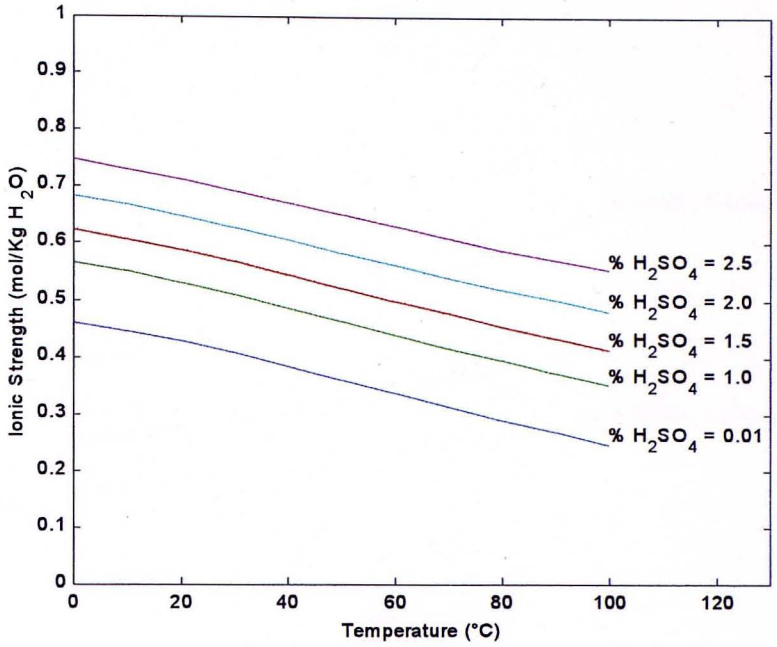

Figure 12. Ionic Strength Versus Temperature – Robinson-Guggenheim-Bates Model

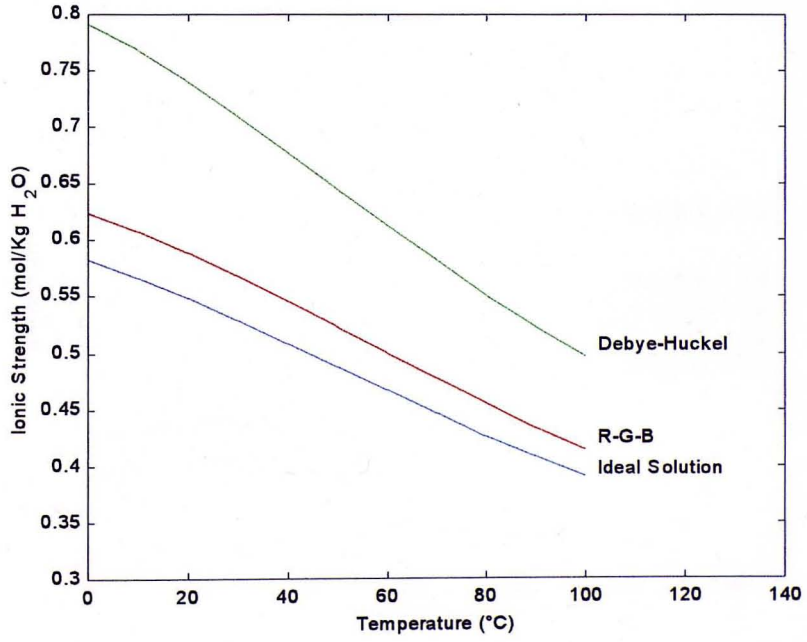

Figure 13. Ionic Strength at 1.5 % H_2SO_4 as a Function of Temperature

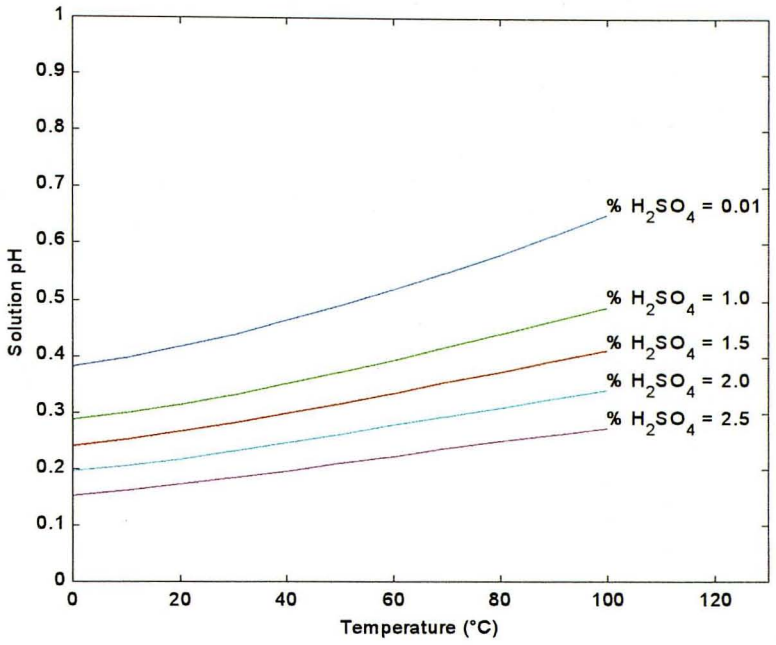

Figure 14. *pH* Versus Temperature – Ideal Solution Model

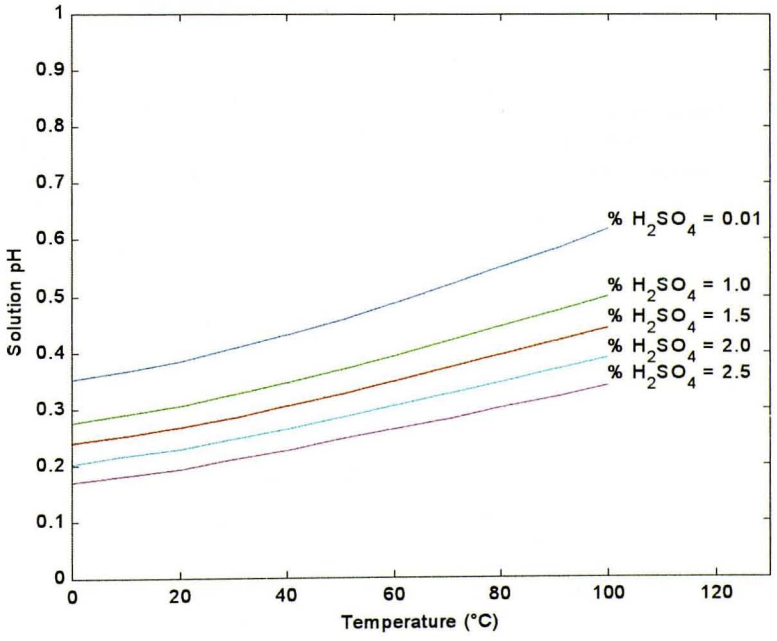

Figure 15. *pH* Versus Temperature – Debye-Hückel Model

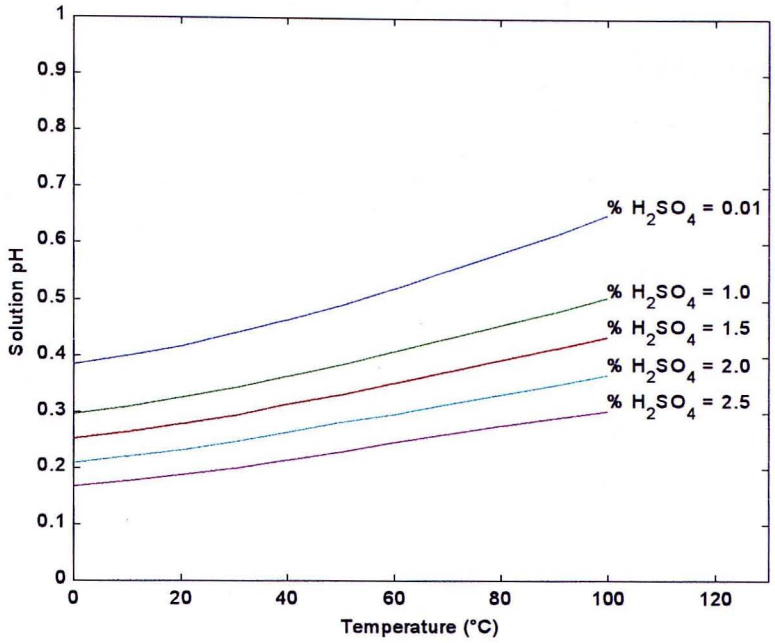

Figure 16. *pH* Versus Temperature – Robinson-Guggenheim-Bates Model

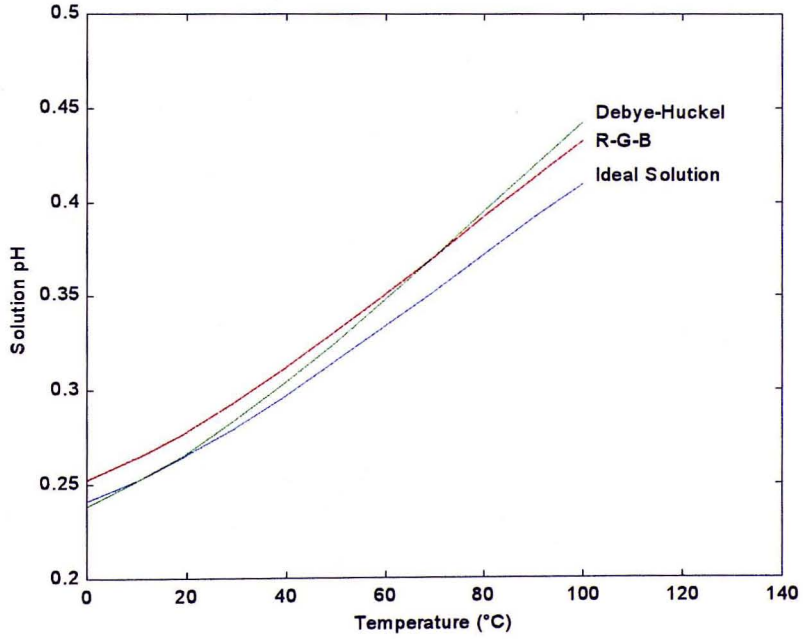

Figure 17. *pH* at 1.5 % H_2SO_4 as a Function of Temperature

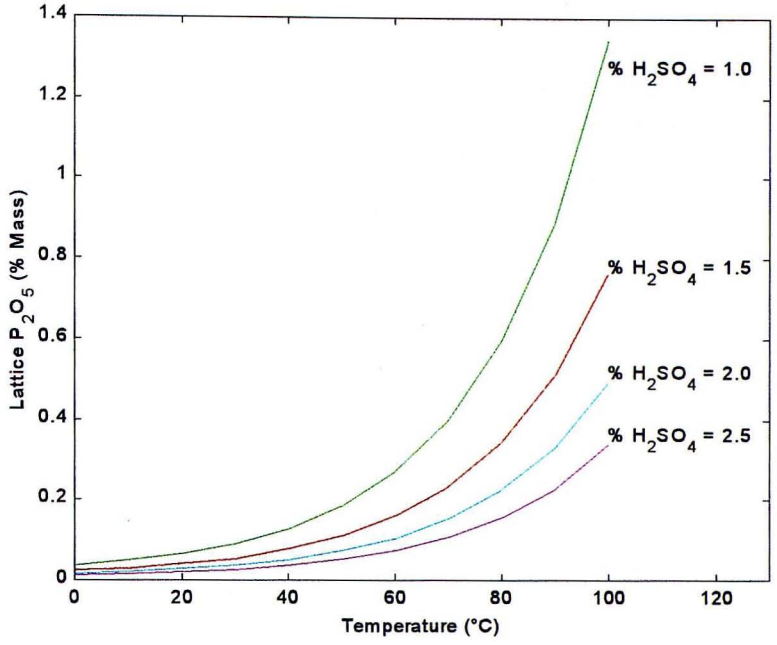

Figure 18. Lattice Loss Versus Temperature – Ideal Solution Model

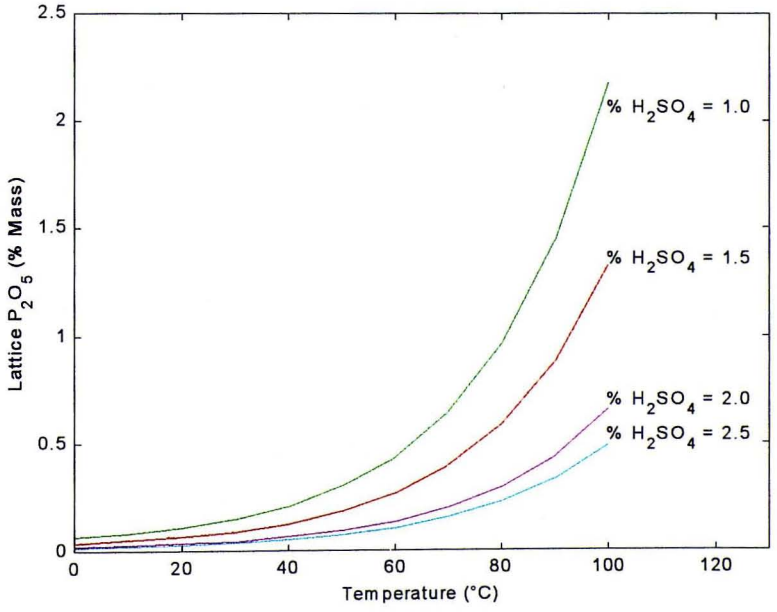

Figure 19. Lattice Loss Versus Temperature – Debye-Hückel Model

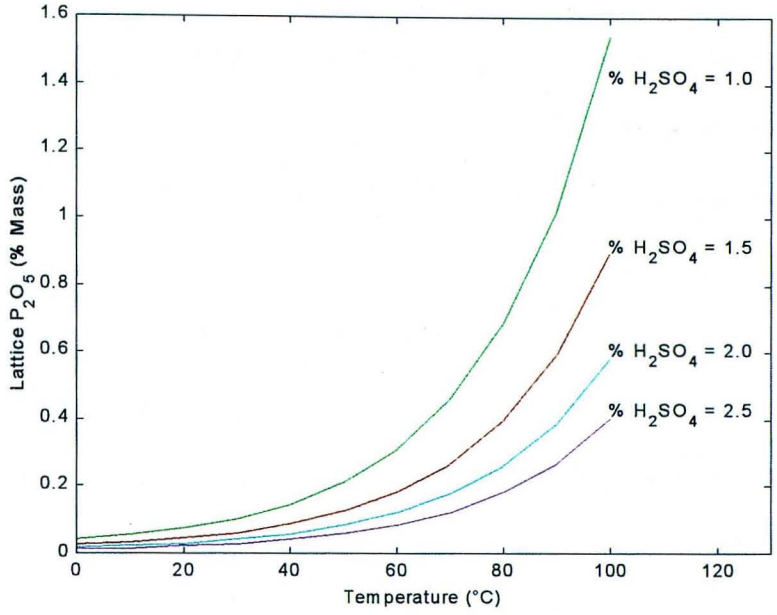

Figure 20. Lattice Loss Versus Temperature – Robinson-Guggenheim-Bates Model

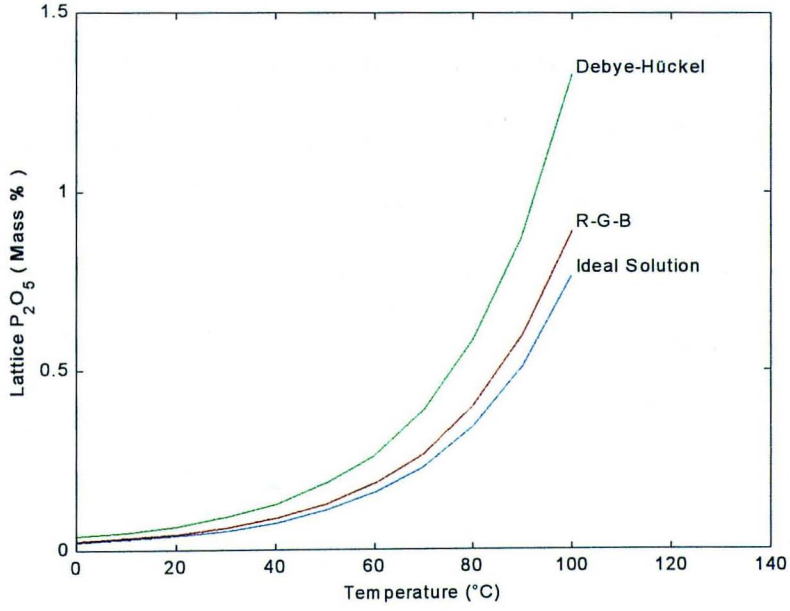

Figure 21. Lattice Loss at 1.5 % H_2SO_4 as a Function of Temperature

4.3 Sulfuric Acid Effect on System Variables

Using sulfuric acid content of the liquid phase as an input list that varied from 0.01 to 2.50 % by mass, the simulation was ran using three different activity coefficient models: ideal solution, Debye-Hückel, and Robinson-Guggenheim-Bates. Each simulation run was carried out with five different inputs of temperature.

Ionic strength increased almost linearly with increasing % H_2SO_4. This result shows that the average degree of ionization, and thus the electrostatic interactions among ions, tends to increase with increasing % H_2SO_4. The ideal solution model predicted the lowest values for ionic strength while the Debye-Hückel model predicted the highest. Robinson-Guggenheim-Bates model predicted intermediate values for ionic strength but closer to those predicted by the ideal solution model. Furthermore, Debye-Hückel and Robinson-Guggenheim-Bates models prediction of ionic strength becomes closer to the ideal solution model prediction as ionic strength value decreases. This is expected since both models reduce to the ideal solution model at an ionic strength of zero.

The liquid phase *pH* decreased linearly with increasing % H_2SO_4. This result shows that the activity, and thus the molality, of the hydrogen ion tend to increase with increasing % H_2SO_4. This observation is in agreement with the previous one concerning ionic strength. As % H_2SO_4 increases, the average degree of ionization increases which will increase the molality and activity of the hydrogen ion. For most of the % H_2SO_4 range, the ideal solution model predicted the lowest values while the Robinson-Guggenheim-Bates model predicted the highest. The Debye-Hückel model on the other hand, predicted intermediate *pH* values between 1.15 and 1.75 % H_2SO_4, lowest *pH* values below 1.15 % H_2SO_4, and highest *pH* values above 1.75 % H_2SO_4.

The phosphate lattice loss decreased significantly with increase in % H_2SO_4. As was shown earlier, sulfuric acid is used to extract phosphoric acid from phosphate rock while gypsum crystals will precipitate as a byproduct. Increasing precipitation of gypsum, due to increasing sulfuric acid concentration, will increase its concentration in the solid solution bringing the solid phase content of DCPD down.

The ideal solution model predicted the lowest values for phosphate lattice loss while the Debye-Hückel model predicted the highest. Robinson-Guggenheim-Bates model predicted intermediate values for phosphate lattice loss but closer to those predicted by the ideal solution model. Furthermore, Debye-Hückel and Robinson-Guggenheim-Bates models prediction of phosphate lattice loss becomes closer to the ideal solution model prediction as % H_2SO_4 increases.

Sulfuric acid dissociates instantaneously forming HSO_4^- and H^+ ions in the liquid phase; therefore, high concentration of sulfuric acid also means high concentrations of HSO_4^- and H^+ ions in the aqueous solution. According to the Equilibrium reactions of the thermodynamic model, increasing concentration of HSO_4^- will increase its dissociation rate to form more SO_4^{2-} ions. Increasing concentration of SO_4^{2-} ions will shift the equilibrium of gypsum towards more precipitation, which will decrease the concentration of Ca^{2+} ions in the aqueous solution. Increasing concentration of H^+ ions due to increasing dissociation of sulfuric acid and HSO_4^- ions will slow down the dissociation of phosphoric acid and $H_2PO_4^-$ ions, which will reduce the concentration of HPO_4^{2-} in the aqueous solution. Decreasing concentrations of Ca^{2+} and HPO_4^{2-} ions will shift the equilibrium of DCPD towards more dissolution and the phosphate losses will decrease as a consequence.

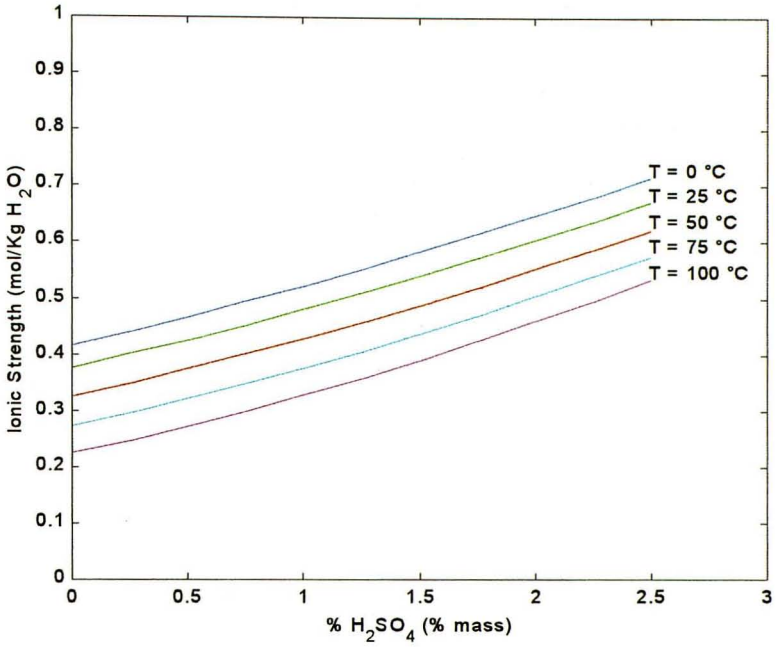

Figure 22. Ionic Strength Versus % H_2SO_4 – Ideal Solution Model

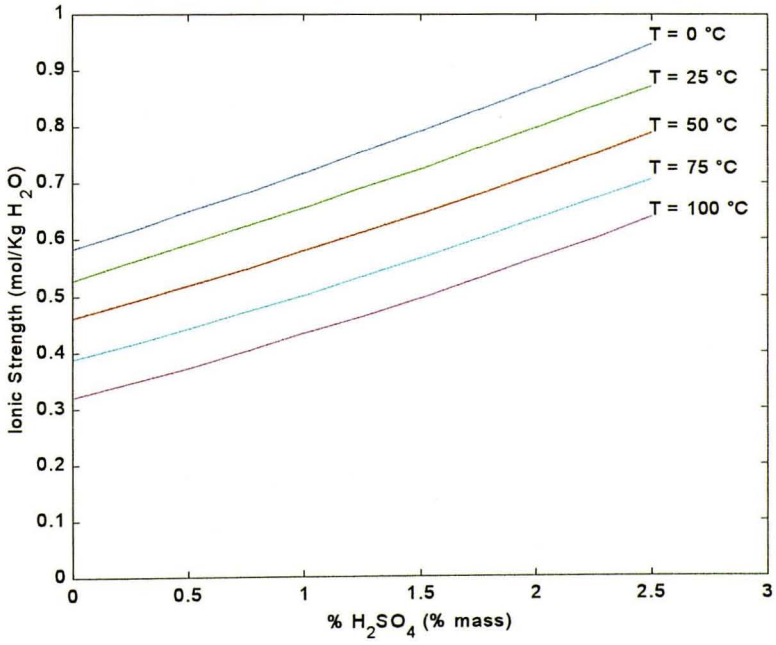

Figure 23. Ionic Strength Versus % H_2SO_4 – Debye-Hückel Model

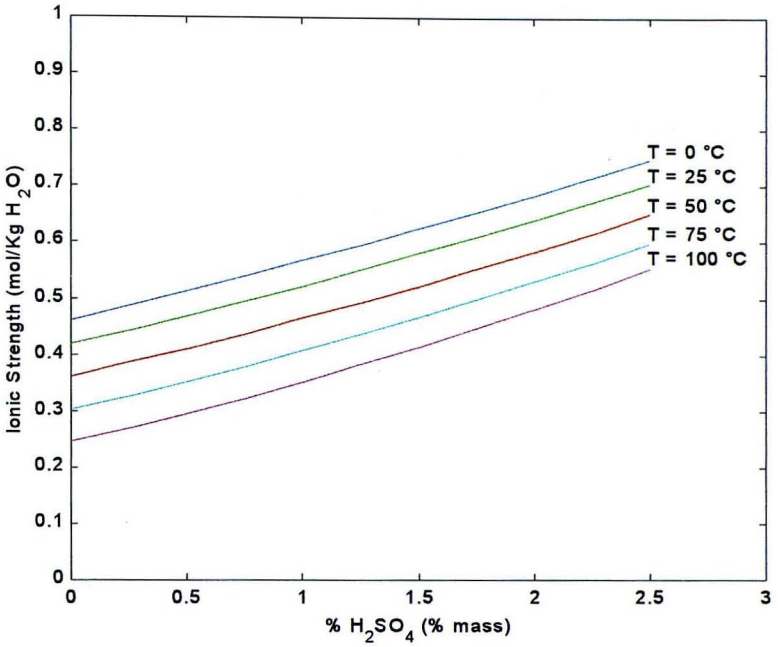

Figure 24. Ionic Strength Versus % H_2SO_4 – Robinson-Guggenheim-Bates Model

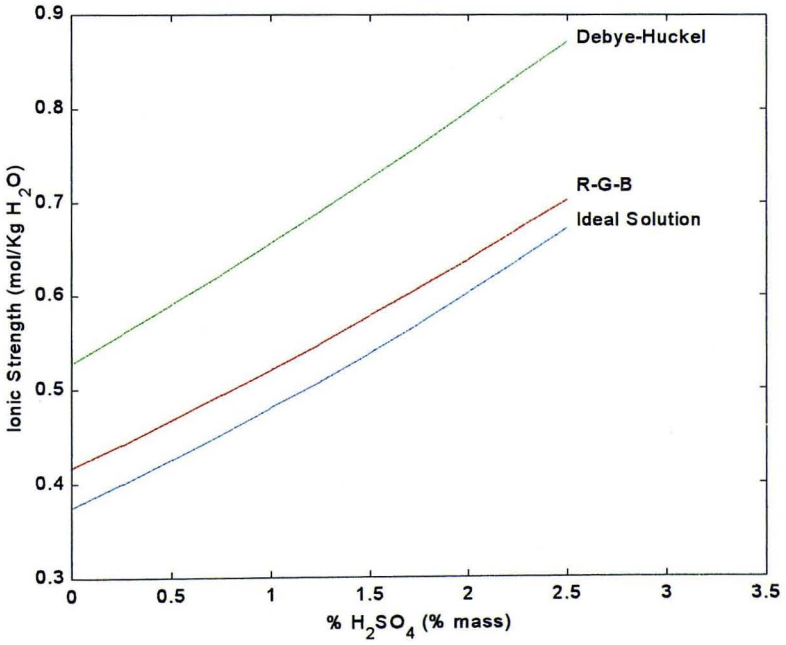

Figure 25. Ionic Strength at 25 °C as a Function of % H_2SO_4

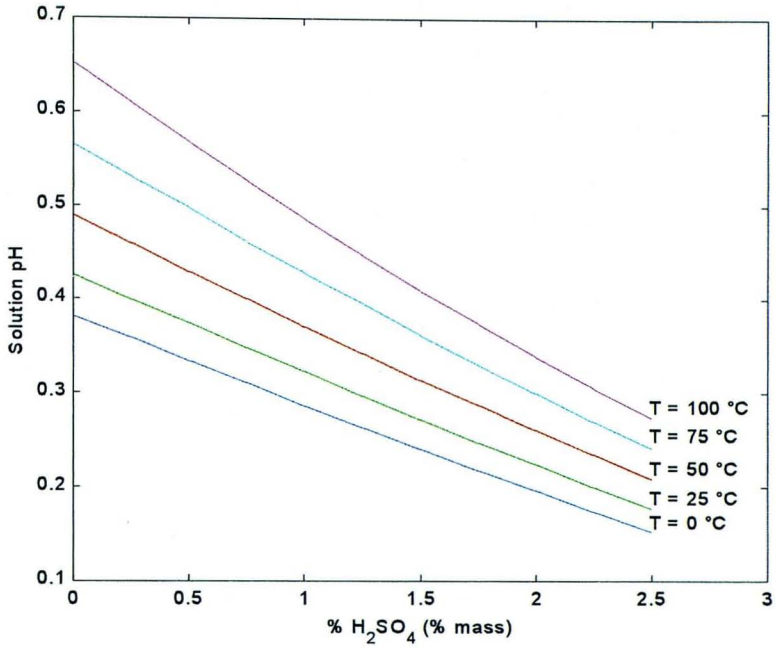

Figure 26. *pH* Versus % H_2SO_4 – Ideal Solution Model

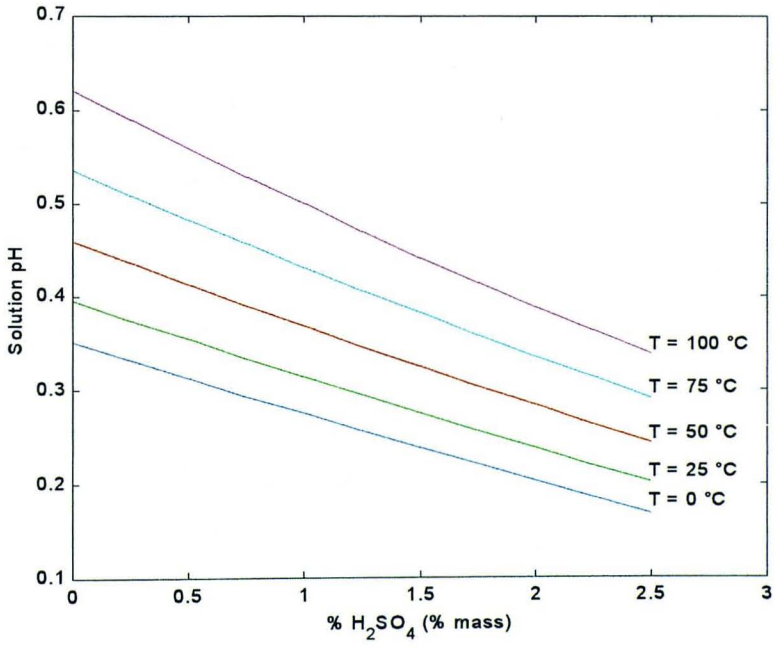

Figure 27. *pH* Versus % H_2SO_4 – Debye-Hückel Model

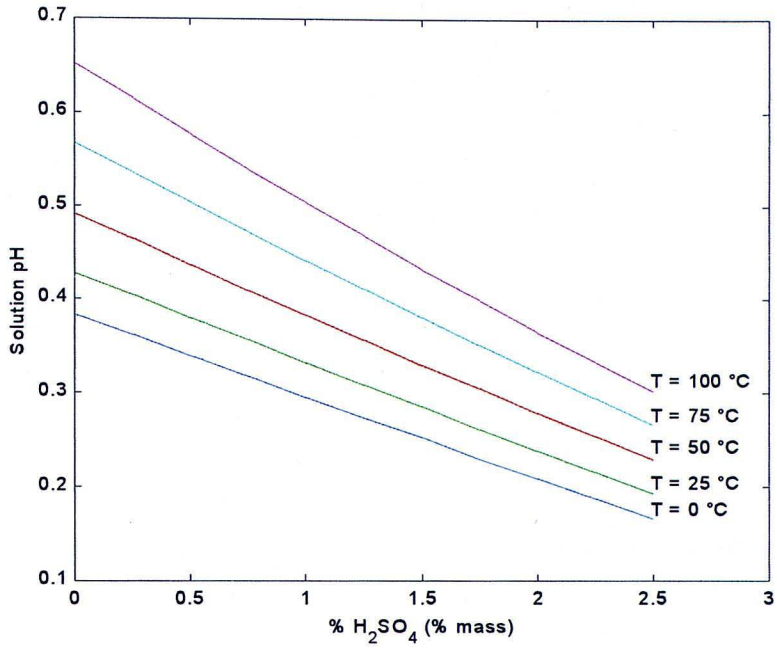

Figure 28. *pH* Versus % H_2SO_4 – Robinson-Guggenheim-Bates Model

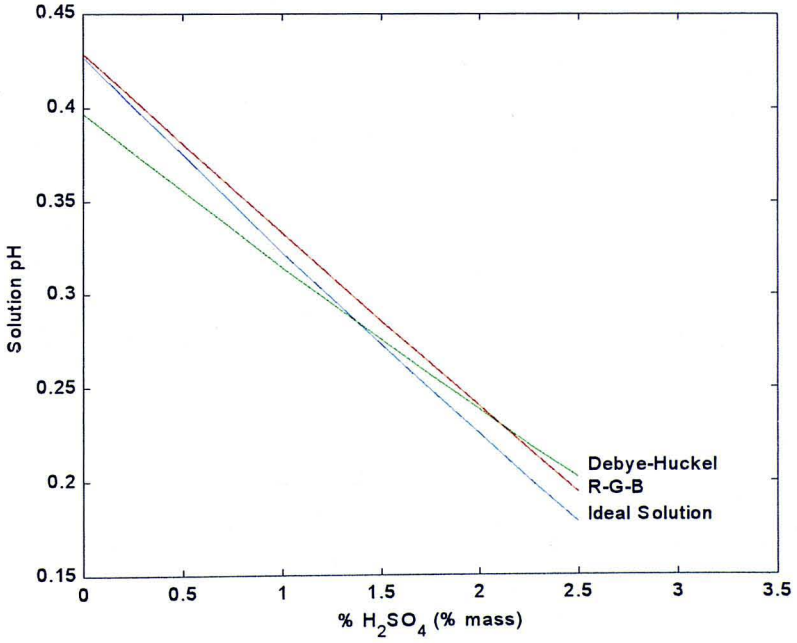

Figure 29. *pH* at 25 °C as a Function of % H_2SO_4

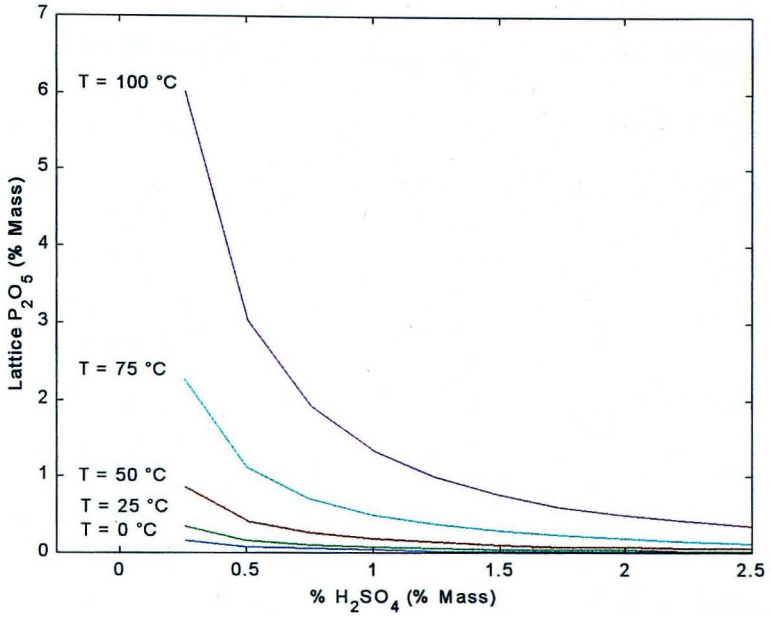

Figure 30. Lattice Loss Versus % H_2SO_4 – Ideal Solution Model

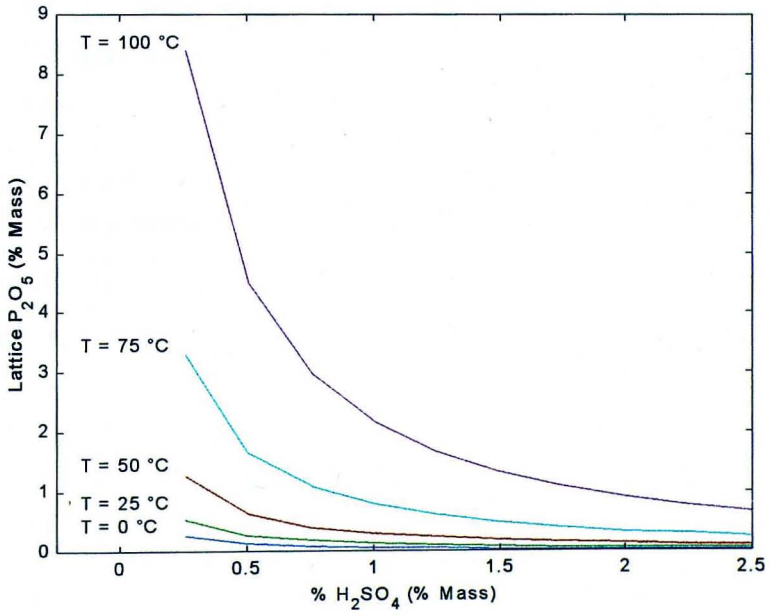

Figure 31. Lattice Loss Versus % H_2SO_4 – Debye-Hückel Model

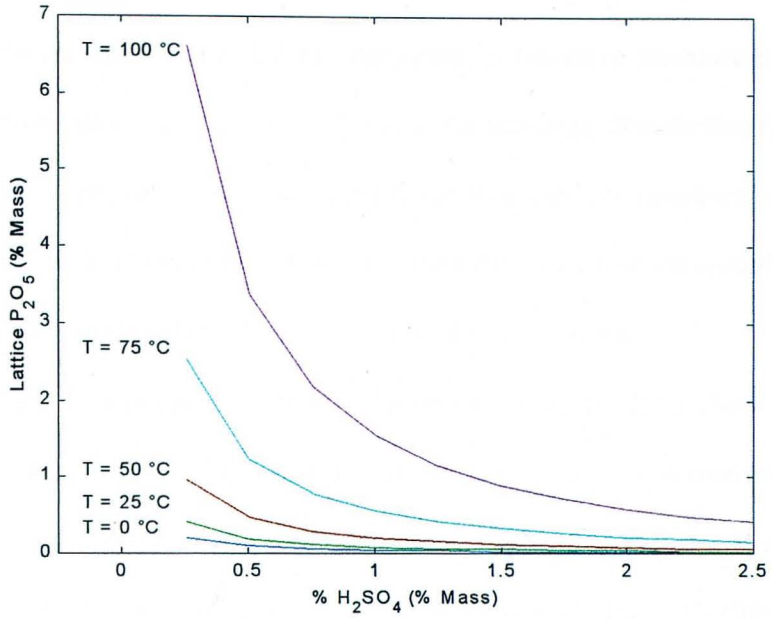

Figure 32. Lattice Loss Versus % H_2SO_4 – Robinson-Guggenheim-Bates Model

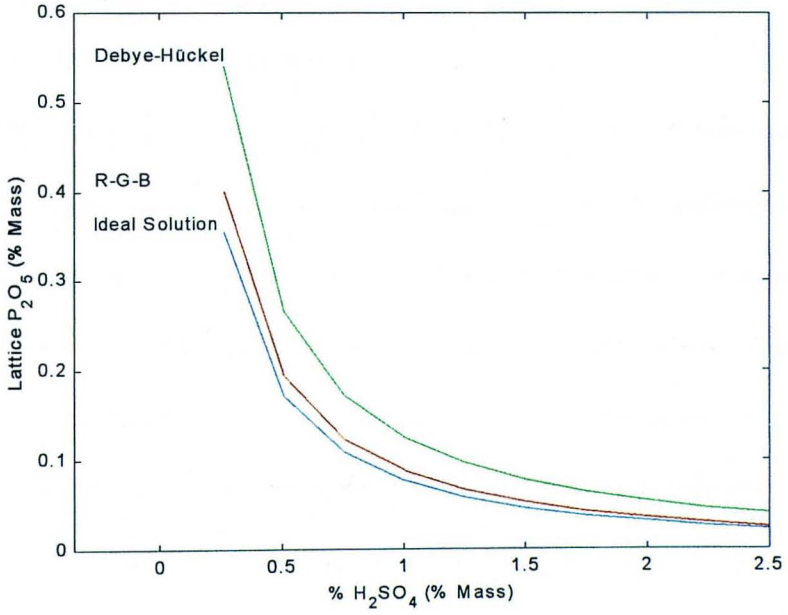

Figure 33. Lattice Loss at 25 °C as a Function of % H_2SO_4

4.4 Model Validation

The model can be validated by comparing its results to literature data. Only two sets of phosphate lattice loss data were found in the literature. The thermodynamic model developed in the previous chapter was used to run two different simulations analogous to the literature data. Simulation results and literature data were then compared to each other to determine the validity of the developed thermodynamic model.

Griffith [14] predicted the DCPD concentrations in the solid phase at a constant temperature of 25 °C and a 28 % liquid content of P_2O_5 for a specified range of liquid phase % H_2SO_4. Griffith employed ideal solution, Debye-Hückel, and Bromley activity coefficient models to compute phosphate losses. Figure 34 shows Griffith's results and Figure 35 shows simulation results when ran at the same conditions. The model predicts slightly more phosphate losses than what Griffith had computed when ideal solution model is employed, but it predicts less phosphate losses than what Griffith had computed when Debye-Hückel model is employed.

Griffith used different values for ΔCp° and ΔH° to estimate the equilibrium constants of model reactions, but that was unimportant since the simulation was run at the reference state temperature of 25 °C which will reduce equation (23) to equation (24) and the values of ΔCp° and ΔH° become irrelevant. The difference between the two predictions, even though minor, can be attributed to different factors. Griffith used different values for the reference state equilibrium constants and solubility products than those used in the simulation. In addition, Griffith assigned a value of unity to the second Debye-Hückel parameter, β, whereas Equation (29), presented earlier in Chapter 2, was used in the simulation to estimate that parameter.

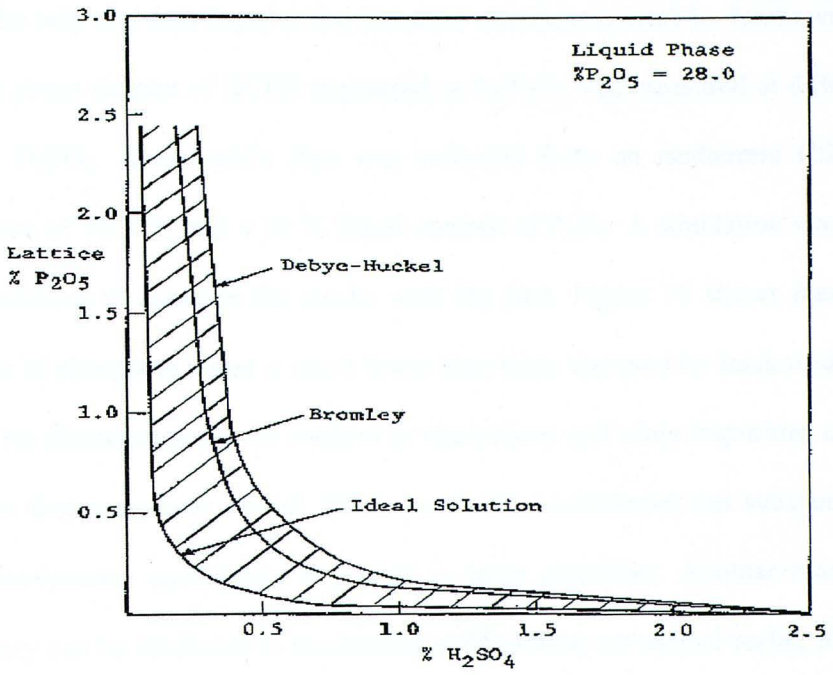

Figure 34. Griffith Prediction of Lattice Loss at 25 °C

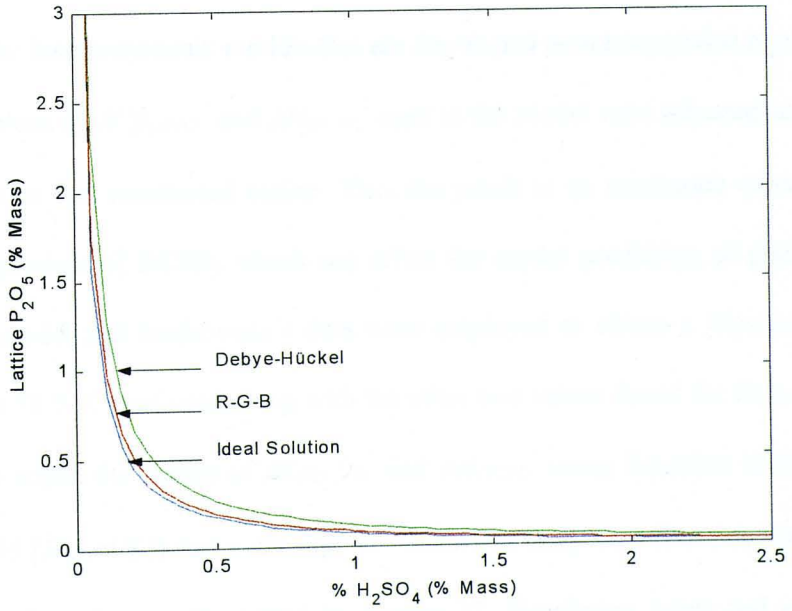

Figure 35. Model Prediction of Lattice Loss at 25 °C

The only real data found in the literature was that reported by Janikowski et al [15]. The solid phase content of DCPD expressed as % P_2O_5 was measured at different liquid phase % H_2SO_4. Janikowski's data was collected from an isothermal CSTR with a temperature of 78.5 °C and a 31 % liquid content of P_2O_5. A simulation was run at the same conditions to compare the results with the data. Figure 36 shows that the model prediction of phosphate losses is much lower than those depicted by Janikowski's data.

This discrepancy can be credited to electrolytes and other impurities unaccounted for by the thermodynamic model. These overlooked substances can substantially affect the thermodynamic equilibrium if present in large quantities. Another reason for this discrepancy can be attributed to mechanical malfunctions mentioned earlier in Chapter 1, e.g. poor filtering and insufficient mixing since Janikowski's data is a real industrial data representing practical circumstances. Busot and Griffith [16] hypothesized that an unattained equilibrium in the reactor would result in greater phosphate losses than predicted by thermodynamic models that are developed assuming global equilibrium.

Values of ΔCp_{DCPD}° and ΔH_{DCPD}° used in the model were adjusted using only two data points as was mentioned earlier. This can result in an inaccurate calculation of the solubility product of DCPD, which can affect the model prediction of phosphate lattice loss. The model and Janikowski's data were employed to obtain a Ksp_{DCPD} at 78.5 °C. Ksp_{DCPD} at 78.5 °C was used along with the other two values found for Ksp_{DCPD} at 25 and 37.5 °C to adjust the values of ΔCp_{DCPD}° and ΔH_{DCPD}° using Equation (23). A ΔCp_{DCPD}° of –1415.45 [J/(mol·K)] and a ΔH_{DCPD}° of +258.55 [J/mol] were found to yield the best fit of Janikowski's data as illustrated by Figure 37. Simulation input and output for the Robinson-Guggenheim-Bates curve in Figure 37 is included in Appendix 8.

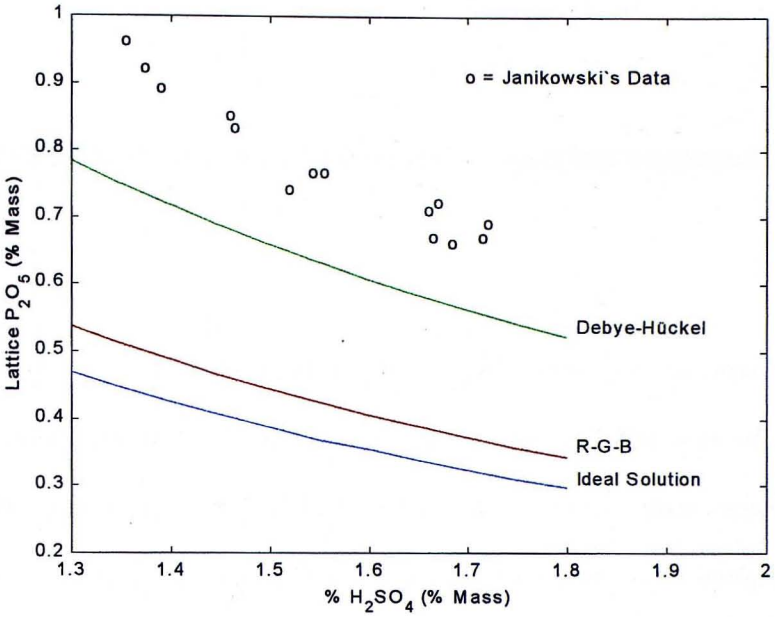

Figure 36. Model Prediction of Lattice Loss at 78.5 °C

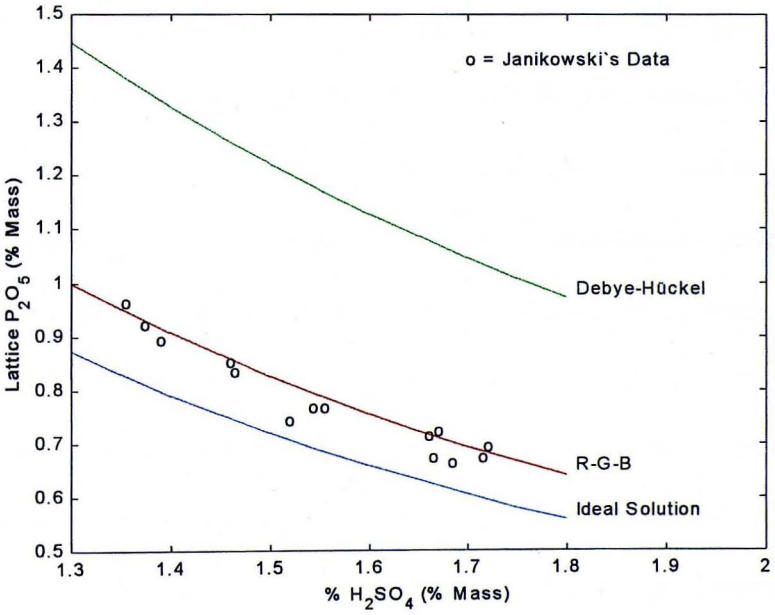

Figure 37. Adjusted Model Prediction of Lattice Loss at 78.5 °C

CHAPTER 5. SUMMARY, CONCLUSION, AND RECOMMENDATIONS

5.1 Summary

Phosphoric acid manufacturing by the dihydrate process involves inevitable phosphate losses due to the formation of gypsum crystals. One type of these losses is triggered by the crystallization of DCPD that has the same lattice structure as that of gypsum. As a result, gypsum and DCPD form a solid solution of a composition that can be controlled thermodynamically.

Thermodynamics of electrolyte solutions such as equilibrium and activity were reviewed. Two relationships, Equations (28) and (29), were developed to estimate the value of the two temperature-dependent Debye-Hückel parameters used in many ionic activity coefficient models. Experimental data of equilibrium constants were regressed to introduce new values of ΔCp° and ΔH° of model reactions to be used in Equation 23 as adjustable parameters (Table 3) to better represent the thermodynamic equilibrium.

A thermodynamic model was developed based upon five equilibrium reactions to predict the limits of distribution of phosphates between the liquid and the solid phases in a reactor used to extract phosphoric acid from rock. Ideal Solution, Debye-Hückel, and Robinson-Guggenheim-Bates electrolyte activity coefficient models were employed alternately to complete the model and to carry out different simulations using several inputs of temperatures and liquid phase sulfuric acid contents. The results were then compared to other literature data to validate the model.

5.2 Conclusion

The developed relationships to estimate the value of the two temperature-dependent Debye-Hückel parameters yielded excellent results that can be shown by Figures 3 and 4. The adjusted fitting parameter values of ΔCp° and ΔH° of model reactions resulted in a more accurate representation of the thermodynamic equilibrium as illustrated by Figures 5 through 9. The adjusted fitting parameter values of ΔCp° and ΔH° for the dissolution of DCPD may not be very reliable since they were obtained by regressing only two experimental data points due to the scarcity of such data.

Decreasing temperature and increasing liquid phase sulfuric acid content was found to minimize phosphate lattice loss. The ideal solution model predicted the lowest values for phosphate lattice loss and the Debye-Hückel model predicted the highest, while Robinson-Guggenheim-Bates model predicted intermediate values. Completing the thermodynamic model with Ideal Solution and Debye-Hückel electrolyte activity coefficient models was found to bind all predictions of phosphate lattice loss.

The model predicts slightly more phosphate losses than what Griffith had computed when ideal solution model is employed, but it predicts less phosphate losses than what Griffith had computed when Debye-Hückel model is employed. Both models assume the formation of an ideal gypsum-DCPD solid solution. The difference between the two predictions can be attributed to different values of equilibrium constants, solubility products, and Debye-Hückel parameters used by Griffith. The model prediction of phosphate losses gave a lower bound to the real industrial data reported by Janikowski. Discrepancy can be accredited to the presence of impurities, mechanical inefficiencies, and unattained equilibrium in addition to the thermodynamically controlled lattice losses.

5.3 Recommendations

The two correlations for the activity coefficients of phosphoric acid and water used in the simulation were determined from vapor pressure data of pure solutions of phosphoric acid and water at 25 °C. The two relationships, Equations (xxxxxv, 62) and (xxxxxvi, 62), incorporate neither the temperature effect nor the effect of the other electrolytes present in the aqueous solution. The activity coefficients of both phosphoric acid and water need to be investigated and more rigorous relationships need to be developed to predict their values.

More research is recommended to identify the most common operating conditions in industry such as the temperature range and the liquid phase content of phosphates and sulfuric acid. Regression calculations and model simulations need to be performed within those operating conditions to better represent real situations. Moreover, more equilibrium data of gypsum and DCPD is needed to perform a more precise regression to adjust the values of ΔCp° and ΔH°.

Finally, sensitivity analyses need to be conducted on the effects of ΔCp°, ΔH°, and other adjusted parameters on phosphate lattice losses. It is also suggested to place a 95% upper and lower confidence limit on the adjusted parameters' prospective figures.

REFERENCES

1. Parker, S. P., 1997, *Dictionary of chemistry*, McGraw-Hill, New York.

2. Van Der Sluis, S., Meszaros, Y., Wesselingh, J. A., and Van Rosmalen, G. M., 1986, *A Clean Technology Phosphoric Acid Process*, The Fertiliser Society, London.

3. Fröchen, J. and Becker, P., 1959, "Crystallization and Co-crystallization in the Manufacture of Wet-Process Phosphoric Acid", *Proceedings of the I. S. M. A. Technical Conference*, No. LE/59/59.

4. Connors, K. A., 1990, *Chemical kinetics*, VCH Publishers, New York.

5. Zemaitis, J. F. Jr., Clark, D. M., Rafal, M., and Scrivner, N. C., 1986, *Handbook of Aqueous Electrolyte Thermodynamics*, American Institute of Chemical Engineers, NewYork.

6. Smith, J. M. and Van Ness, H. C., 1987, *Introduction to Chemical Engineering Thermodynamics*, Fourth Edition, McGraw-Hill, New York.

7. Dean, J. A., 1992, *Lange's Handbook of Chemistry*, Fourteenth Edition, McGraw-Hill, New York.

8. Marshall, W. L., Slusher, R., and Jones, E. V.,1963, "Aqueous Systems at High Temperature. XIV", *Journal of Chemical and Engineering Data*.

9. Patel, P. R., Gregory, T. M., and Brown, W. E., 1974, "Solubility of $CaHPO_4 \cdot 2H_2O$ in the Quaternary System $Ca(OH)_2$-H_3PO_4-NaCl-H_2O at 25 °C", *Journal of Research*, National Bureau of Standards, 78A(6), pp. 675-681.

10. Moreno, E. C. and Gregory, T. M., 1966, "Solubility of $CaHPO_4 \cdot 2H_2O$ and Formation of Ion Pairs in the System $Ca(OH)_2$-H_3PO_4-H_2O at 37.5 °C", *Journal of Research*, National Bureau of Standards, 70A(6), pp. 545-552.

11. Atkins, P. W., 1994, *Physical Chemistry*, Fifth Edition, W. H. Freeman and Company, New York.

12. Lewis, G. N. and Randall, M., 1961, *Thermodynamics*, Second Edition, McGraw-Hill, New York.

13. Franks, F., 1973, *Water*, Plenum Press, London.

14. Griffith, D. J. Jr., 1985, Thermodynamic Bounds on Composition of Calcium Sulfate-Calcium Phosphate Solid Solutions in Equilibrium with Phosphoric Acid Solutions, M. S. Thesis, University of South Florida, Tampa, Florida.

15. Janikowski, S. M., Robinson, N., and Sheldrick, W. F., 1961, "Insoluble Phosphate Losses in Phosphoric Acid Manufacture by the Wet Process", *Proceedings of the Fertilizer Society*, No. 81.

16. Busot, J. C. and Griffith, J., 1987, "Thermodynamic Bounds and Composition of Calcium Sulfate-Calcium Phosphate Solid Solutions in Acid Equilibrium with Phosphoric Acid Solutions", *Proceedings of the Second International Conference on Thermodynamics of Aqueous Electrolyte Solutions*, Warrenton, Virginia.

APPENDICES

Appendix 1. Literature and Experimental Data

Table 4. Debye-Hückel Parameters Data

T (°C)	$A^{(7)}$	$\beta^{(7)}$
0	0.4918	0.3248
5	0.4952	0.3256
10	0.4989	0.3264
15	0.5028	0.3273
20	0.5070	0.3282
25	0.5115	0.3291
30	0.5161	0.3301
35	0.5211	0.3312
40	0.5262	0.3323
45	0.5317	0.3334
50	0.5373	0.3346
55	0.5432	0.3358
60	0.5494	0.3371
65	0.5558	0.3384
70	0.5625	0.3397
75	0.5695	0.3411
80	0.5767	0.3426
85	0.5842	0.3440
90	0.5920	0.3456
95	0.6001	0.3471
100	0.6086	0.3488

Table 5. Equilibrium Constants and Solubility Products at Various Temperatures

T (°C)	$K_{HSO4}^{(7)}$	$K_{H3PO4}^{(7)}$	$K_{H2PO4}^{(7)}$	$K_{Gypsum}^{(8)}$	$K_{DCPD}^{(9)(10)}$
0	0.016672	0.00879	0.486407		
4.3	0.015417				
5		0.008453	0.522396		
10		0.008166	0.557186		
15	0.012764	0.007816	0.587489		
20		0.007464	0.612350		
25	0.010304	0.007112	0.633870	4.22E-05	2.51E-07
30	0.008913	0.006745	0.647143	4.36E-05	
35	0.008035	0.006368	0.653131		
37.5					2.19E-07
40	0.006761	0.005970	0.659174	4.25E-05	
50	0.005675	0.005284	0.656145		
60				3.57E-05	

Appendix 1. (Continued)

Table 6. Physical and Reference State Properties

	MW [7] (Kg / mole)	$Cp°$ [7] [11] [12] [13] (J / mol K)	$H°$ [7] (J / mol)	$G°$ [7] (J / mol)	Z (e)	r [7] (Å)
P_2O_5	0.141945					NA
H_2SO_4	0.098080					NA
H_2O	0.018015	75.35	-285830	-237140		NA
H_3PO_4	0.097995	65	-1288340	-1142650		NA
H_2PO_4	0.096987	-90	-1296290	-1130390	-1	4
HPO_4	0.095979	-316	-1292140	-1089260	-2	4
HSO_4	0.097072	-84	-887340	-755910	-1	4
SO_4	0.096064	-293	-909270	-744530	-2	4
H	0.001008	0	0	0	+1	9
Ca	0.040078	-37	-542830	-553540	+2	6
Gypsum	0.172172	186	-2022600	-1797500		NA
DCPD	0.172088	197	-2403580	-2154750		NA

Table 7. Janikowski's Data

% H_2SO_4	% P_2O_5
1.350	0.960
1.370	0.920
1.385	0.890
1.455	0.850
1.460	0.830
1.515	0.740
1.540	0.765
1.550	0.765
1.655	0.710
1.660	0.670
1.665	0.720
1.680	0.660
1.710	0.670
1.715	0.690

Appendix 2. Matlab Code for Regression of A and β Literature Data

```
T = [0 5 10 15 20 25 30 35 40 45 50 55 60 65 70 75 80 85 90 95 100] ' ;

A = [0.4918 0.4952 0.4989 0.5028 0.5070 0.5115 0.5161 0.5211 0.5262 0.5317 ...
0.5373 0.5432 0.5494 0.5558 0.5625 0.5695 0.5767 0.5842 0.5920 0.6001 0.6086] ' ;

B = [0.3248 0.3256 0.3264 0.3273 0.3282 0.3291 0.3301 0.3312 0.3323 0.3334 ...
0.3346 0.3358 0.3371 0.3384 0.3397 0.3411 0.3426 0.3440 0.3456 0.3471 0.3488] ' ;

TK = T + 273.15 ;

polyfit(TK,A,2)
ans =
0.00000513495200  -0.00215443376623   0.69725708453699

polyfit(TK,B,2)
ans =
0.00000088002615  -0.00032917648667   0.34905962443669

Ar = (0.69725708453699)-(0.00215443376623).*(TK)+(0.00000513495200).*(TK).^2 ;

Br = (0.34905962443669)-(0.00032917648667).*(TK)+(0.00000088002615).*(TK).^2 ;

plot(T,A,'ko',T,Ar,'k-'),xlabel('Temperature(°C)'),ylabel('Parameter A')
gtext('o = data'),gtext('— = fit')

plot(T,B,'ko',T,Br,'k-'),xlabel('Temperature(°C)'),ylabel('Parameter Beta')
gtext('o = data'),gtext('— = fit')
```

Appendix 3. Matlab Code for Regression of K_{HSO4} Experimental Data

```
R = 8.314 ;
Tr = 298.15 ;
T = [273.15 277.45 288.15 298.15 303.15 308.15 313.15 323.15] ' ;
pK_HSO4 = [1.778 1.812 1.894 1.987 2.050 2.095 2.170 2.246] ' ;
K_HSO4 = 10 .^ ( - pK_HSO4 ) ;

% Global Variables, Initial Guesses, & Options

global T K_HSO4 ;
parameters =[-21930 -209] ;
OPTIONS(1) = 0 ;

% The Fun Function ( An m-File )

        % function f = fun(parameters) ;
        % global T K_HSO4 ;
        % Delta_H_HSO4 = parameters(1,1) ;
        % Delta_Cp_HSO4 = parameters(1,2) ;
        % Kc_HSO4 = 0.01030386120442 .* exp ( -(Delta_H_HSO4/R).*((1./T)-...
        %                 (1/Tr)) - (Delta_Cp_HSO4/R).*(log(Tr./T)-(Tr./T)+1) ) ;
        % f = sum((Kc_HSO4-K_HSO4).^2) ;

% Regression & Results, Kc_HSO4 = Calculated Equilibrium Constant

x = fmins('fun(x)',parameters,OPTIONS);
Delta_H_HSO4 = x(1,1) ;
ans = -1.692832807144829e+004 ;
Delta_Cp_HSO4 = x(1,2) ;
ans = -3.100073820743674e+002 ;
Delta_Hr_HSO4 = -21930 ;
Delta_Cpr_HSO4 = -209 ;

Kc1_HSO4 = 0.01030386120442 .* exp ( -(Delta_H_HSO4/R).*((1./T)-(1/Tr)) - ...
                (Delta_Cp_HSO4/R).*(log(Tr./T)-(Tr./T)+1) ) ;

Kc2_HSO4 = 0.01030386120442 .* exp ( -(Delta_Hr_HSO4/R).*((1./T)-(1/Tr)) - ...
                (Delta_Cpr_HSO4/R).*(log(Tr./T)-(Tr./T)+1) ) ;

plot(T-273.15,K_HSO4,'ko',T-273.15,Kc1_HSO4,'k:',T-273.15,Kc2_HSO4,'k-'),...
xlabel('Temperature (°C)'),ylabel('K_H_S_O_4_^- (mol/Kg H_2O)'),...
title('K_H_S_O_4_^- Versus T'),...
gtext('o  = data'),gtext('^.^.^.^. = regression'),gtext('— = literature')
```

Appendix 4. Matlab Code for Regression of K_{H3PO4} Experimental Data

```
R = 8.314 ;
Tr = 298.15 ;
T = [273.15 278.15 283.15 288.15 293.15 298.15 303.15 308.15 313.15 323.15] ' ;
pK_H3PO4 = [2.056 2.073 2.088 2.107 2.127 2.148 2.171 2.196 2.224 2.277] ' ;
K_H3PO4 = 10 .^ ( - pK_H3PO4 ) ;

% Global Variables, Initial Guesses, & Options

global T K_H3PO4 ;
parameters =[-7950 -155] ;
OPTIONS(1) = 0 ;

% The Fun Function ( An m-File )

        % function f = fun(parameters) ;
        % global T K_H3PO4 ;
        % Delta_H_H3PO4 = parameters(1,1) ;
        % Delta_Cp_H3PO4 = parameters(1,2) ;
        % Kc_H3PO4 = 0.00711213513653 .* exp ( -(Delta_H_H3PO4/R).*((1./T)-...
        %                 (1/Tr)) - (Delta_Cp_H3PO4/R).*(log(Tr./T)-(Tr./T)+1) ) ;
        % f = sum((Kc_H3PO4-K_H3PO4).^2) ;

% Regression & Results, Kc_H3PO4 = Calculated Equilibrium Constant

x = fmins('fun(x)',parameters,OPTIONS) ;
Delta_H_H3PO4 = x(1,1) ;
ans = -7.663321868430035e+003 ;
Delta_Cp_H3PO4 = x(1,2) ;
ans = -1.554144573028516e+002 ;
Delta_Hr_H3PO4 = -7950 ;
Delta_Cpr_H3PO4 = -155 ;

Kc1_H3PO4 = 0.00711213513653 .* exp ( -(Delta_H_H3PO4/R).*((1./T)-(1/Tr)) - ...
                (Delta_Cp_H3PO4/R).*(log(Tr./T)-(Tr./T)+1) );

Kc2_H3PO4 = 0.00711213513653 .* exp ( -(Delta_Hr_H3PO4/R).*((1./T)-(1/Tr)) - ...
                (Delta_Cpr_H3PO4/R).*(log(Tr./T)-(Tr./T)+1) );

plot(T-273.15,K_H3PO4,'ko',T-273.15,Kc1_H3PO4,'k:',T-273.15,Kc2_H3PO4,'k-'),...
xlabel('Temperature (°C)'),ylabel('K_H_3_P_O_4 (mol/Kg H_2O)'),...
title('K_H_3_P_O_4 Versus T'),...
gtext('o  = data'),gtext('^.^.^.^. = regression'),gtext('— = literature')
```

Appendix 5. Matlab Code for Regression of K_{H2PO4} Experimental Data

```
R = 8.314 ;
Tr = 298.15 ;
T = [273.15 278.15 283.15 288.15 293.15 298.15 303.15 308.15 313.15 323.15] ' ;
pK_H2PO4 = [7.313 7.282 7.254 7.231 7.213 7.198 7.189 7.185 7.181 7.183] ' ;
K_H2PO4 = 10 .^ ( - pK_H2PO4 ) ;

% Global Variables, Initial Guesses, & Options

global T K_H2PO4 ;
parameters = [4150 -226] ;
OPTIONS(1) = 0 ;

% The Fun Function ( An m-File )

        % function f = fun(parameters) ;
        % global T K_H2PO4 ;
        % Delta_H_H2PO4 = parameters(1,1) ;
        % Delta_Cp_H2PO4 = parameters(1,2) ;
        % Kc_H2PO4 = 6.338697112569273e-8 .*exp ( -(Delta_H_H2PO4/R).*((1./T)-...
        %                 (1/Tr)) - (Delta_Cp_H2PO4/R).*(log(Tr./T)-(Tr./T)+1) ) ;
        % f = sum((Kc_H2PO4-K_H2PO4).^2) ;

% Regression & Results, Kc_H2PO4 = Calculated Equilibrium Constant

x = fmins('fun(x)',parameters,OPTIONS) ;
Delta_H_H2PO4 = x(1,1) ;
ans = 4.033524375681814e+003 ;
Delta_Cp_H2PO4 = x(1,2) ;
ans = -2.489728900252766e+002 ;
Delta_Hr_H2PO4 = 4150 ;
Delta_Cpr_H2PO4 = -226 ;

Kc1_H2PO4 = 6.338697112569273e-8 .*exp (-(Delta_H_H2PO4/R).*((1./T)-(1/Tr)) - ...
                (Delta_Cp_H2PO4/R).*(log(Tr./T)-(Tr./T)+1) ) ;

Kc2_H2PO4 = 6.338697112569273e-8 .*exp (-(Delta_Hr_H2PO4/R).*((1./T)-(1/Tr)) - ...
                (Delta_Cpr_H2PO4/R).*(log(Tr./T)-(Tr./T)+1) ) ;

plot(T-273.15,K_H2PO4,'ko',T-273.15,Kc1_H2PO4,'k:',T-273.15,Kc2_H2PO4,'k-'),...
xlabel('Temperature (°C)'),ylabel('K_H_2_P_O_4_^- (mol/Kg H_2O)'),...
title('K_H_2_P_O_4_^- Versus T'),...
gtext('o  = data'),gtext('^.^.^.^. = regression'),gtext('— = literature')
```

Appendix 6. Matlab Code for Regression of K_{Gypsum} Experimental Data

```
R = 8.314 ;
Tr = 298.15 ;
T = [298.15 303.15 313.15 333.15] ' ;
K_Gypsum = [42.2e-6 43.6e-6 42.5e-6 35.7e-6] ' ;

% Global Variables, Initial Guesses, & Options

global T K_Gypsum ;
parameters = [-1160 -365.3] ;
OPTIONS(1) = 0 ;

% The Fun Function ( An m-File )

        % function f = fun(parameters) ;
        % global T K_Gypsum ;
        % Delta_H_Gypsum = parameters(1,1) ;
        % Delta_Cp_Gypsum = parameters(1,2) ;
        % Kc_Gypsum = 42.2e-6 .* exp ( -(Delta_H_Gypsum/R).*((1./T)-(1/Tr)) - ...
        %                 (Delta_Cp_Gypsum/R).*(log(Tr./T)-(Tr./T)+1) ) ;
        % f = sum((Kc_Gypsum-K_Gypsum).^2) ;

% Regression & Results, Kc_Gypsum = Calculated Solubility Product

x = fmins('fun(x)',parameters,OPTIONS) ;
Delta_H_Gypsum = x(1,1) ;
ans = 4.338149706356578e+003 ;
Delta_Cp_Gypsum = x(1,2) ;
ans = -4.935892366111605e+002 ;
Delta_Hr_Gypsum = -1160 ;
Delta_Cpr_Gypsum = -365.3 ;

Kc1_Gypsum = 42.2e-6 .* exp ( -(Delta_H_Gypsum/R).*((1./T)-(1/Tr)) - ...
                (Delta_Cp_Gypsum/R).*(log(Tr./T)-(Tr./T)+1) ) ;

Kc2_Gypsum = 42.2e-6 .* exp ( -(Delta_Hr_Gypsum/R).*((1./T)-(1/Tr)) - ...
                (Delta_Cpr_Gypsum/R).*(log(Tr./T)-(Tr./T)+1) ) ;

plot(T-273.15,K_Gypsum,'ko',T-273.15,Kc1_Gypsum,'k:',T-273.15,Kc2_Gypsum,'k-'),...
xlabel('Temperature (°C)'),ylabel('K_G_y_p_s_u_m (mol/Kg H_2O)^4'),...
title('K_G_y_p_s_u_m Versus T'),...
gtext('o  = data'),gtext('^.^.^.^. = regression'),gtext('— = literature')
```

Appendix 7. Matlab Code for Regression of K_{DCPD} Experimental Data

```
R = 8.314 ;
Tr = 298.15 ;
T = [298.15 310.65] ' ;
K_DCPD = [2.512663370009572e-7 2.19e-7] ' ;

% Global Variables, Initial Guesses, & Options

global T K_DCPD ;
Delta_Cp_DCPD = [-399.3] ;
OPTIONS(1) = 0 ;

% The Fun Function ( An m-File )

        % function f = fun(Delta_Cp_DCPD) ;
        % global T K_DCPD ;
        % Kc_DCPD = 2.512663370009572e-7 .* exp ( -(-3050/R).*((1./T)-(1/Tr)) -...
        %                 (Delta_Cp_DCPD/R).*(log(Tr./T)-(Tr./T)+1) ) ;
        % f = sum((Kc_DCPD-K_DCPD).^2) ;

% Regression & Results, Kc_DCPD = Calculated Solubility Product

Delta_Cp_DCPD = fmins('fun(x)',Delta_Cp_DCPD,OPTIONS) ;
ans = -8.787345583534251e+002 ;
Delta_Cpr_DCPD = -399.3 ;

Kc1_DCPD = 2.512663370009572e-7 .* exp ( -(-3050/R).*((1./T)-(1/Tr)) - ...
                (Delta_Cp_DCPD/R).*(log(Tr./T)-(Tr./T)+1) );

Kc2_DCPD = 2.512663370009572e-7 .* exp ( -(-3050/R).*((1./T)-(1/Tr)) - ...
                (Delta_Cpr_DCPD/R).*(log(Tr./T)-(Tr./T)+1) );

plot(T-273.15,K_DCPD,'ko',T-273.15,Kc1_DCPD,'k:',T-273.15,Kc2_DCPD,'k-'),...
xlabel('Temperature (°C)'),ylabel('K_D_C_P_D (mol/Kg H_2O)^4'),...
title('K_D_C_P_D Versus T'),...
gtext('o  = data'),gtext('^.^.^.^. = regression'),gtext('— = literature')
```

Appendix 8. TK Solver Code of Thermodynamic Model

```
; Liquid phase properties

TPM = m_H3PO4 + m_H2PO4 + m_HPO4
TSM = m_HSO4 + m_SO4
%P2O5 = (TPMΘ_P2O5 MW_P2O5 ϕ_H2O) • 100
%H2SO4 = (TSMΘ_H2SO4 MW_H2SO4 ϕ_H2O) • 100
ϕ_H2O = M_H2O / M_Total
m_H2O = 1 / MW_H2O

; Total mass balance in the liquid phase

M_TPM = m_H3PO4 MW_H3PO4 + m_H2PO4 MW_H2PO4 + m_HPO4 MW_HPO4
M_TSM = m_HSO4 MW_HSO4 + m_SO4 MW_SO4
M_Other = m_H MW_H + m_Ca MW_Ca
M_Total = M_H2O + M_TPM + M_TSM + M_Other

; Electroneutrality

z_H2PO4 m_H2PO4 + z_HPO4 m_HPO4 + z_HSO4 m_HSO4 + z_SO4 m_SO4 + z_H m_H + z_Ca m_Ca = 0

; Phenomenological assumptions

; 1) Liquid phase acid equilibria

K_HSO4 = a_SO4 a_H / a_HSO4
K_H3PO4 = a_H2PO4 a_H / a_H3PO4
K_H2PO4 = a_HPO4 a_H / a_H2PO4

; 2) Solid-liquid equilibria

Ksp_Gypsum = a_SO4 a_Ca a_H2O^2 / x_Gypsum
Ksp_DCPD = a_HPO4 a_Ca a_H2O^2 / x_DCPD
x_Gypsum + x_DCPD = 1

; Solid phase properties

ω_DCPD = x_DCPD MW_DCPD / (x_Gypsum MW_Gypsum + x_DCPD MW_DCPD)
%P2O5s = [ω_DCPD [1 / MW_DCPD] Ψ_P2O5 MW_P2O5] • 100
```

Appendix 8. (Continued)

; Temperature-dependent equilibrium constants

$$K\_HSO4 = Kr\_HSO4\, e^{\left[\frac{-\Delta H\_HSO4}{R}\left[\frac{1}{T}-\frac{1}{Tr}\right]-\frac{\Delta Cp\_HSO4}{R}\left[\ln\left[\frac{Tr}{T}\right]-\frac{Tr}{T}+1\right]\right]}$$

$$K\_H3PO4 = Kr\_H3PO4\, e^{\left[\frac{-\Delta H\_H3PO4}{R}\left[\frac{1}{T}-\frac{1}{Tr}\right]-\frac{\Delta Cp\_H3PO4}{R}\left[\ln\left[\frac{Tr}{T}\right]-\frac{Tr}{T}+1\right]\right]}$$

$$K\_H2PO4 = Kr\_H2PO4\, e^{\left[\frac{-\Delta H\_H2PO4}{R}\left[\frac{1}{T}-\frac{1}{Tr}\right]-\frac{\Delta Cp\_H2PO4}{R}\left[\ln\left[\frac{Tr}{T}\right]-\frac{Tr}{T}+1\right]\right]}$$

$$Ksp\_Gypsum = Kspr\_Gypsum\, e^{\left[\frac{-\Delta H\_Gypsum}{R}\left[\frac{1}{T}-\frac{1}{Tr}\right]-\frac{\Delta Cp\_Gypsum}{R}\left[\ln\left[\frac{Tr}{T}\right]-\frac{Tr}{T}+1\right]\right]}$$

$$Ksp\_DCPD = Kspr\_DCPD\, e^{\left[\frac{-\Delta H\_DCPD}{R}\left[\frac{1}{T}-\frac{1}{Tr}\right]-\frac{\Delta Cp\_DCPD}{R}\left[\ln\left[\frac{Tr}{T}\right]-\frac{Tr}{T}+1\right]\right]}$$

; Reference state equilibrium constants

$$Kr\_HSO4 = e^{\left[\frac{-\Delta Gr\_HSO4}{RTr}\right]}$$

$$Kr\_H3PO4 = e^{\left[\frac{-\Delta Gr\_H3PO4}{RTr}\right]}$$

$$Kr\_H2PO4 = e^{\left[\frac{-\Delta Gr\_H2PO4}{RTr}\right]}$$

$$Kspr\_Gypsum = e^{\left[\frac{-\Delta Gr\_Gypsum}{RTr}\right]}$$

$$Kspr\_DCPD = e^{\left[\frac{-\Delta Gr\_DCPD}{RTr}\right]}$$

; Reference state heat capacities of reaction

$$\Delta Cpr\_HSO4 = Cpr\_SO4 + Cpr\_H - Cpr\_HSO4$$
$$\Delta Cpr\_H3PO4 = Cpr\_H2PO4 + Cpr\_H - Cpr\_H3PO4$$
$$\Delta Cpr\_H2PO4 = Cpr\_HPO4 + Cpr\_H - Cpr\_H2PO4$$
$$\Delta Cpr\_Gypsum = Cpr\_Ca + Cpr\_SO4 + 2Cpr\_H2O - Cpr\_Gypsum$$
$$\Delta Cpr\_DCPD = Cpr\_Ca + Cpr\_HPO4 + 2Cpr\_H2O - Cpr\_DCPD$$

; Reference state enthalpies of reaction

$$\Delta Hr\_HSO4 = Hr\_SO4 + Hr\_H - Hr\_HSO4$$
$$\Delta Hr\_H3PO4 = Hr\_H2PO4 + Hr\_H - Hr\_H3PO4$$
$$\Delta Hr\_H2PO4 = Hr\_HPO4 + Hr\_H - Hr\_H2PO4$$
$$\Delta Hr\_Gypsum = Hr\_Ca + Hr\_SO4 + 2Hr\_H2O - Hr\_Gypsum$$
$$\Delta Hr\_DCPD = Hr\_Ca + Hr\_HPO4 + 2Hr\_H2O - Hr\_DCPD$$

Appendix 8. (Continued)

; Reference state Gibbs free energies of reaction

$$\Delta Gr\_HSO4 = Gr\_SO4 + Gr\_H - Gr\_HSO4$$
$$\Delta Gr\_H3PO4 = Gr\_H2PO4 + Gr\_H - Gr\_H3PO4$$
$$\Delta Gr\_H2PO4 = Gr\_HPO4 + Gr\_H - Gr\_H2PO4$$
$$\Delta Gr\_Gypsum = Gr\_Ca + Gr\_SO4 + 2Gr\_H2O - Gr\_Gypsum$$
$$\Delta Gr\_DCPD = Gr\_Ca + Gr\_HPO4 + 2Gr\_H2O - Gr\_DCPD$$

; Defining activities

$$a\_H2O = m\_H2O\gamma\_H2O$$
$$a\_H3PO4 = m\_H3PO4\,\gamma\_H3PO4$$
$$a\_H2PO4 = m\_H2PO4\,\gamma\_H2PO4$$
$$a\_HPO4 = m\_HPO4\,\gamma\_HPO4$$
$$a\_HSO4 = m\_HSO4\,\gamma\_HSO4$$
$$a\_SO4 = m\_SO4\,\gamma\_SO4$$
$$a\_H = m\_H\gamma\_H$$
$$a\_Ca = m\_Ca\gamma\_Ca$$

; Defining solution's ionic strength and pH

$$I = \frac{1}{2}\left[m\_H2PO4\ z\_H2PO4^{2} + m\_HPO4\ z\_HPO4^{2} + m\_HSO4\ z\_HSO4^{2} + m\_SO4\ z\_SO4^{2} + \ldots \right.$$
$$\left. \ldots + m\_H\ z\_H^{2} + m\_Ca\ z\_Ca^{2} \right]$$

$$pH = -\log(a\_Hp\_H2O)$$

; Non-electrolyte activity coefficients

$$\gamma\_H2O = -(0.87979) + (0.75533\ \%P2O5) - \left[0.0012084\ \%P2O5^{2} \right] + \left[\frac{15.258}{\%P2O5} \right]$$
$$\gamma\_H3PO4 = (22.676) - (1.0192\ \%P2O5) + \left[0.01891\ \%P2O5^{2} \right] - \left[\frac{159.56}{\%P2O5} \right]$$

; Electrolyte activity coefficients

; a) Ideal solution model

$$\gamma\_H2PO4 = 1$$
$$\gamma\_HPO4 = 1$$
$$\gamma\_HSO4 = 1$$
$$\gamma\_SO4 = 1$$
$$\gamma\_H = 1$$
$$\gamma\_Ca = 1$$

; b) Debye-Huckel model

$$A = (0.69725708453699) - (0.00215443376623)T + (0.00000513495200)T^{2}$$
$$\beta = (0.34905962443669) - (0.00032917648667)T + (0.00000088002615)T^{2}$$

Appendix 8. (Continued)

$$\gamma\_H2PO4 = 10^{-\left[\frac{Az\_H2PO4^2 \, I^{0.5}}{1 + \left[\beta r\_H2PO4 \, I^{.5}\right]}\right]}$$

$$\gamma\_HPO4 = 10^{-\left[\frac{Az\_HPO4^2 \, I^{0.5}}{1 + \left[\beta r\_HPO4 \, I^{.5}\right]}\right]}$$

$$\gamma\_HSO4 = 10^{-\left[\frac{Az\_HSO4^2 \, I^{0.5}}{1 + \left[\beta r\_HSO4 \, I^{.5}\right]}\right]}$$

$$\gamma\_SO4 = 10^{-\left[\frac{Az\_SO4^2 \, I^{0.5}}{1 + \left[\beta r\_SO4 \, I^{.5}\right]}\right]}$$

$$\gamma\_H = 10^{-\left[\frac{Az\_H^2 \, I^{0.5}}{1 + \left[\beta r\_HI^{.5}\right]}\right]}$$

$$\gamma\_Ca = 10^{-\left[\frac{Az\_Ca^2 \, I^{0.5}}{1 + \left[\beta r\_CaI^{.5}\right]}\right]}$$

; c) Robinson-Guggenheim-Bates model

$$\gamma\_H2PO4 = 10^{-\left[\left[\frac{.511I}{1 + 1.5I} - (.2I)\right] z\_H2PO4^2\right]}$$

$$\gamma\_HPO4 = 10^{-\left[\left[\frac{.511I}{1 + 1.5I} - (.2I)\right] z\_HPO4^2\right]}$$

$$\gamma\_HSO4 = 10^{-\left[\left[\frac{.511I}{1 + 1.5I} - (.2I)\right] z\_HSO4^2\right]}$$

$$\gamma\_SO4 = 10^{-\left[\left[\frac{.511I}{1 + 1.5I} - (.2I)\right] z\_SO4^2\right]}$$

$$\gamma\_H = 10^{-\left[\left[\frac{.511I}{1 + 1.5I} - (.2I)\right] z\_H^2\right]}$$

$$\gamma\_Ca = 10^{-\left[\left[\frac{.511I}{1 + 1.5I} - (.2I)\right] z\_Ca^2\right]}$$

Appendix 8. (Continued)

```
; Programming: list guess

TPM = place ( 'TPM , elt() + 1)
TSM = place ( 'TSM , elt() + 1)
ϕ_H2O = place ( 'ϕ_H2O , elt() + 1)
pH = place ( 'pH , elt() + 1)
I = place ( 'I , elt() + 1)
x_DCPD = place ( 'x_DCPD , elt() + 1)
M_Total = place ( 'M_Total , elt() + 1)
m_HSO4 = place ( 'm_HSO4 , elt() + 1)
m_SO4 = place ( 'm_SO4 , elt() + 1)
m_H = place ( 'm_H , elt() + 1)
γ_HSO4 = place ( 'γ_HSO4 , elt() + 1)
γ_SO4 = place ( 'γ_SO4 , elt() + 1)
γ_H = place ( 'γ_H , elt() + 1)
```

Status	Input	Name	Output	Unit	Comment Program input & output for RGB curve in Figure 37
	8.314	R		J / mol K	ideal gas constant
	298.15	Tr		K	reference temperature
	351.65	T		K	reactor's temperature
LGuess	7.814255438	TPM		mol / Kg H2O	Total Phosphate Molality
LGuess	.2371261531	TSM		mol / Kg H2O	Total Sulfate Molality
	31	%P2O5		% mass	% P2O5 equivalence by mass (Kg P2O5 / Kg Sol)
L	1.3	%H2SO4		% mass	% H2SO4 equivalence by mass (Kg H2SO4 / Kg Sol)
L		%P2O5s	1.000000931	% mass	% P2O5 equivalence by mass in the solid phase
	.5	Θ_P2O5		mol / mol	mol of P2O5 equivalence / mol of TPM
	1	Θ_H2SO4		mol / mol	mol of H2SO4 equivalence / mol of TSM
	.5	Ψ_P2O5		mol / mol	mol of P2O5 equivalence / mol of DCPD
	.997	ρ_H2O		Kg H2O / L	reference state density of water
LGuess	.5589657664	ϕ_H2O		mass fraction	weight fraction of water in the liquid
L		ω_DCPD	.0242472289	mass fraction	DCPD mass fraction in solid solution
LGuess	.505546421	I		mol / L	ionic strength, I = 0.5 Σ [m_i (z_i) ^ 2]
LGuess	.3447376327	pH			pH of solution
L		A	.5746269037		Debye-Huckel constant , valid @ 0 - 100 °C
L		β	.3421267367		Debye-Huckel constant , valid @ 0 - 100 °C
L		x_Gypsum	.9757412226	mol fraction	gypsum mole fraction in solid solution
LGuess	.0242587774	x_DCPD		mol fraction	DCPD mole fraction in solid solution
	1	M_H2O		Kg / Kg H2O	mass of water / mass of water
L		M_TPM	.7654937577	Kg / Kg H2O	mass of TPM / mass of water
L		M_TSM	.0230165961	Kg / Kg H2O	mass of TSM / mass of water
L		M_Other	.0005079727	Kg / Kg H2O	mass of other species / mass of water
LGuess	1.789018327	M_Total		Kg / Kg H2O	mass of solution / mass of water

Appendix 8. (Continued)

Status	Input	Name	Output	Unit	Comment
	4	r_H2PO4		A°	effective ionic radius
	4	r_HPO4		A°	effective ionic radius
	4	r_HSO4		A°	effective ionic radius
	4	r_SO4		A°	effective ionic radius
	9	r_H		A°	effective ionic radius
	6	r_Ca		A°	effective ionic radius
	.1419446	MW_P2O5		Kg / mole	molecular weight of phosphate equivalence
	.0980796	MW_H2SO4		Kg / mole	molecular weight of sulfuric acid equivalence
	.0180154	MW_H2O		Kg / mole	molecular weight of water
	.0979954	MW_H3PO4		Kg / mole	molecular weight of phosphoric acid
	.0969874	MW_H2PO4		Kg / mole	molecular weight of phosphate dihydrate ion
	.0959794	MW_HPO4		Kg / mole	molecular weight of hydrated phosphate ion
	.0970716	MW_HSO4		Kg / mole	molecular weight of hydrated sulfate ion
	.0960636	MW_SO4		Kg / mole	molecular weight of sulfate ion
	.001008	MW_H		Kg / mole	molecular weight of hydrogen ion
	.040078	MW_Ca		Kg / mole	molecular weight of calcium ion
	.172172	MW_Gypsum		Kg / mole	molecular weight of gypsum
	.172088	MW_DCPD		Kg / mole	molecular weight of DCPD
	-1	z_H2PO4			Charge of phosphate dihydrate ion
	-2	z_HPO4			Charge of sulfate dihydrate ion
	-1	z_HSO4			Charge of sulfate hydrate ion
	-2	z_SO4			Charge of sulfate ion
	1	z_H			Charge of hydrogen ion
	2	z_Ca			Charge of calcium ion
		m_H2O	55.50806532	mol / Kg H2O	molality of water
L		m_H3PO4	7.549047485	mol / Kg H2O	molality of phosphoric acid
L		m_H2PO4	.2652079088	mol / Kg H2O	molality of phosphate dihydrate ion
L		m_HPO4	4.427943E-8	mol / Kg H2O	molality of sulfate dihydrate ion
LGuess	.2355200522	m_HSO4		mol / Kg H2O	molality of sulfate hydrate ion
LGuess	.0016061009	m_SO4		mol / Kg H2O	molality of sulfate ion
LGuess	.5039402022	m_H		mol / Kg H2O	molality of hydrogen ion
L		m_Ca	2.455495E-8	mol / Kg H2O	molality of calcium ion
		a_H2O	1213.759403	mol / Kg H2O	activity of water
L		a_H3PO4	30.99799863	mol / Kg H2O	activity of phosphoric acid
L		a_H2PO4	.2386572731	mol / Kg H2O	activity of phosphate dihydrate ion
L		a_HPO4	2.90372E-8	mol / Kg H2O	activity of sulfate dihydrate ion
L		a_HSO4	.2119415431	mol / Kg H2O	activity of sulfate hydrate ion
L		a_SO4	.0010532359	mol / Kg H2O	activity of sulfate ion
L		a_H	.4534894719	mol / Kg H2O	activity of hydrogen ion
L		a_Ca	1.610244E-8	mol / Kg H2O	activity of calcium ion
		γ_H2O	21.86636115		activity coefficient of water
		γ_H3PO4	4.106213226		activity coefficient of phosphoric acid
		γ_H2PO4	.8998874666		activity coefficient of phosphate dihydrate ion
		γ_HPO4	.6557719142		activity coefficient of sulfate dihydrate ion
Guess	.8998874666	γ_HSO4			activity coefficient of sulfate hydrate ion
Guess	.6557719142	γ_SO4			activity coefficient of sulfate ion
Guess	.8998874666	γ_H			activity coefficient of hydrogen ion
		γ_Ca	.6557719142		activity coefficient of calcium ion
	75.35	Cpr_H2O		J / mol K	reference state heat capacity of water
	65	Cpr_H3PO4		J / mol K	reference state heat capacity of phosphoric acid
	-90	Cpr_H2PO4		J / mol K	reference state heat capacity of phosphate dihydrate ion
	-316	Cpr_HPO4		J / mol K	reference state heat capacity of sulfate dihydrate ion
	-84	Cpr_HSO4		J / mol K	reference state heat capacity of sulfate hydrate ion
	-293	Cpr_SO4		J / mol K	reference state heat capacity of sulfate ion
	0	Cpr_H		J / mol K	reference state heat capacity of hydrogen ion
	-37	Cpr_Ca		J / mol K	reference state heat capacity of calcium ion
	186	Cpr_Gypsum		J / mol K	reference state heat capacity of gypsum
	197	Cpr_DCPD		J / mol K	reference state heat capacity of DCPD

Appendix 8. (Continued)

Status	Input	Name	Output	Unit	Comment
	-285830	Hr_H2O		J / mol	reference state enthalpy of water
	-1288340	Hr_H3PO4		J / mol	reference state enthalpy of phosphoric acid
	-1296290	Hr_H2PO4		J / mol	reference state enthalpy of phosphate dihydrate ion
	-1292140	Hr_HPO4		J / mol	reference state enthalpy of sulfate dihydrate ion
	-887340	Hr_HSO4		J / mol	reference state enthalpy of sulfate hydrate ion
	-909270	Hr_SO4		J / mol	reference state enthalpy of sulfate ion
	0	Hr_H		J / mol	reference state enthalpy of hydrogen ion
	-542830	Hr_Ca		J / mol	reference state enthalpy of calcium ion
	-2022600	Hr_Gypsum		J / mol	reference state enthalpy of gypsum
	-2403580	Hr_DCPD		J / mol	reference state enthalpy of DCPD
	-237140	Gr_H2O		J / mol	reference state Gibbs free energy of water
	-1142650	Gr_H3PO4		J / mol	reference state Gibbs free energy of phosphoric acid
	-1130390	Gr_H2PO4		J / mol	reference state Gibbs free energy of phosphate dihydrate ion
	-1089260	Gr_HPO4		J / mol	reference state Gibbs free energy of sulfate dihydrate ion
	-755910	Gr_HSO4		J / mol	reference state Gibbs free energy of sulfate hydrate ion
	-744530	Gr_SO4		J / mol	reference state Gibbs free energy of sulfate ion
	0	Gr_H		J / mol	reference state Gibbs free energy of hydrogen ion
	-553540	Gr_Ca		J / mol	reference state Gibbs free energy of calcium ion
	-1797500	Gr_Gypsum		J / mol	reference state Gibbs free energy of gypsum
	-2154750	Gr_DCPD		J / mol	reference state Gibbs free energy of DCPD
		ΔCpr_HSO4	-209	J / mol K	reference state heat capacity of HSO4 dissolution
		ΔCpr_H3PO4	-155	J / mol K	reference state heat capacity of H3PO4 dissolution
		ΔCpr_H2PO4	-226	J / mol K	reference state heat capacity of H2PO4 dissolution
		ΔCpr_Gypsum	-365.3	J / mol K	reference state heat capacity of gypsum solubility
		ΔCpr_DCPD	-399.3	J / mol K	reference state heat capacity of DCPD solubility
		ΔHr_HSO4	-21930	J / mol	reference state enthalpy of HSO4 dissolution
		ΔHr_H3PO4	-7950	J / mol	reference state enthalpy of H3PO4 dissolution
		ΔHr_H2PO4	4150	J / mol	reference state enthalpy of H2PO4 dissolution
		ΔHr_Gypsum	-1160	J / mol	reference state enthalpy of gypsum solubility
		ΔHr_DCPD	-3050	J / mol	reference state enthalpy of DCPD solubility
		ΔGr_HSO4	11380	J / mol	reference state Gibbs free energy of HSO4 dissolution
		ΔGr_H3PO4	12260	J / mol	reference state Gibbs free energy of H3PO4 dissolution
		ΔGr_H2PO4	41130	J / mol	reference state Gibbs free energy of H2PO4 dissolution
		ΔGr_Gypsum	25150	J / mol	reference state Gibbs free energy of gypsum solubility
		ΔGr_DCPD	37670	J / mol	reference state Gibbs free energy of DCPD solubility
	-310.007382	ΔCp_HSO4		J / mol K	adjusted reference state heat capacity of HSO4 dissolution
	-155.414457	ΔCp_H3PO4		J / mol K	adjusted reference state heat capacity of H3PO4 dissolution
	-248.97289	ΔCp_H2PO4		J / mol K	adjusted reference state heat capacity of H2PO4 dissolution
	-493.589237	ΔCp_Gypsum		J / mol K	adjusted reference state heat capacity of gypsum solubility
	-1415.45	ΔCp_DCPD		J / mol K	adjusted reference state heat capacity of DCPD solubility
	-16928.3281	ΔH_HSO4		J / mol	adjusted reference state enthalpy of HSO4 dissolution
	-7663.32187	ΔH_H3PO4		J / mol	adjusted reference state enthalpy of H3PO4 dissolution
	4033.524376	ΔH_H2PO4		J / mol	adjusted reference state enthalpy of H2PO4 dissolution
	4338.149706	ΔH_Gypsum		J / mol	adjusted reference state enthalpy of gypsum solubility
	258.55	ΔH_DCPD		J / mol	adjusted reference state enthalpy of DCPD solubility
	.0103038612	Kr_HSO4		mol / Kg H2O	reference state equilibrium constant of HSO4 dissolution
	.0071121351	Kr_H3PO4		mol / Kg H2O	reference state equilibrium constant of H3PO4 dissolution
	6.338697E-8	Kr_H2PO4		mol / Kg H2O	reference state equilibrium constant of H2PO4 dissolution
	.0000422	Kspr_Gypsum		(mol / Kg H2O)^ 4	reference state solubility product of gypsum
	2.512663E-7	Kspr_DCPD		(mol / Kg H2O)^ 4	reference state solubility product of DCPD
L		K_HSO4	.0022535996	mol / Kg H2O	equilibrium constant of HSO4 dissolution
L		K_H3PO4	.0034914693	mol / Kg H2O	equilibrium constant of H3PO4 dissolution
L		K_H2PO4	5.517563E-8	mol / Kg H2O	equilibrium constant of H2PO4 dissolution
L		Ksp_Gypsum	2.560637E-5	(mol / Kg H2O)^ 4	solubility product of gypsum
L		Ksp_DCPD	2.839507E-8	(mol / Kg H2O)^ 4	solubility product of DCPD